

Neural Concept Binder

Wolfgang Stammer^{1,2,*}

Antonia Wüst^{1,*}

David Steinmann^{1,*}

Kristian Kersting^{1,2,3,4}

¹Computer Science Department, TU Darmstadt; ²Hessian Center for AI (hessian.AI);

³German Research Center for AI (DFKI); ⁴Centre for Cognitive Science, TU Darmstadt

Abstract

The challenge in object-based visual reasoning lies in generating descriptive yet distinct concept representations. Moreover, doing this in an unsupervised fashion requires human users to understand a model’s learned concepts and potentially revise false concepts. In addressing this challenge, we introduce the *Neural Concept Binder*, a new framework for deriving discrete concept representations resulting in what we term “concept-slot encodings”. These encodings leverage both “soft binding” via object-centric block-slot encodings and “hard binding” via retrieval-based inference. The Neural Concept Binder facilitates straightforward concept inspection and direct integration of external knowledge, such as human input or insights from other AI models like GPT-4. Additionally, we demonstrate that incorporating the hard binding mechanism does not compromise performance; instead, it enables seamless integration into both neural and symbolic modules for intricate reasoning tasks, as evidenced by evaluations on our newly introduced CLEVR-Sudoku dataset.¹

1 Introduction

An essential aspect of visual reasoning is obtaining a proper *conceptual* understanding of the world by learning visual concepts and processing these into a suitable representation (*cf.* Fig. 1). The majority of current machine learning (ML) approaches that focus on visual concept-based processing utilize forms of supervised [28, 59, 26], weakly-supervised [34, 60, 41, 54, 4, 72] or text-guided [23] learning of concepts. These approaches all require some form of additional (prior) knowledge about the relevant domain. An attractive alternative, though much more challenging, is to learn concepts in an unsupervised fashion. This comes with several challenges: (i) learning an expressive concept representation without concept supervision is intrinsically difficult [33], and (ii) there is no guarantee that learned concepts align with general domain knowledge [30, 75, 5] and can therefore be utilized for complex downstream tasks. Moreover, (iii) to trust that the learned concept representations are reliable for high stakes scenarios [10], it is necessary to make the model’s concept representations human-*inspectable* and -*revisable* [59, 60, 25] (*cf.* Fig. 1).

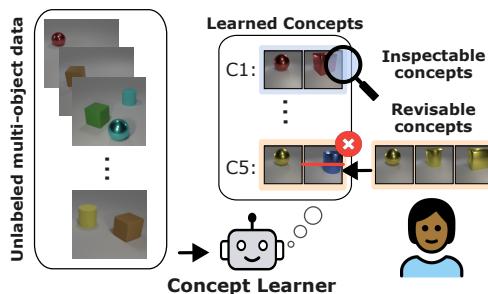


Figure 1: **Unsupervised learning of concepts for visual reasoning.** Models that learn concepts from unlabeled data require inspectable and revisable concept representations.

¹Code and data available here.

*These authors share equal contribution.

Correspondence to: Wolfgang Stammer <wolfgang.stammer@cs.tu-darmstadt.de>.

These challenges raise questions about the nature of the unsupervised learned concept representations. Continuous encodings [51, 50, 68, 70] are easier to learn and more expressive. However, they are difficult to interpret and suffer from problems related to poor generalization [71] and information leakage [40, 42]. On the other hand, discrete encodings [60, 70, 20, 2] are hard to learn [37, 63, 5], but are easier to understand and thus align, *e.g.*, to a task at hand.

This work proposes the **Neural Concept Binder** (NCB) framework to learn expressive yet inspectable and revisable concepts from unlabeled data. NCB combines continuous encodings, obtained via block-slot-based *soft-binding*, with discrete concept representations, obtained via retrieval-based *hard-binding*. Thus, to tackle the challenges of unsupervised concept learning, NCB harnesses the advantages of continuous *and* discrete concept representations. Moreover, NCB features a straightforward inspection of learned concepts and facilitates easy revision procedures to align the obtained concept knowledge, *e.g.*, with prior knowledge. In our evaluations, we show that NCB’s discrete *concept-slot* encodings retain the expressiveness of their continuous counterparts. Furthermore, they can easily be used in downstream applications via symbolic *and* transparent neural computations. In this context we introduce our novel *CLEVR-Sudoku* dataset that represents a challenging visual puzzle requiring both perception and reasoning capabilities (*cf.* Fig. 4).

In summary, our contributions are the following: **(i)** we introduce the Neural Concept Binder framework (NCB) for unsupervised concept learning, **(ii)** we show the possibilities to integrate NCB with symbolic and subsymbolic modules in challenging downstream tasks, achieving performance on par with supervised trained models, **(iii)** we highlight the possibilities of easy concept inspection and revision via NCB, and **(iv)** we introduce the novel *CLEVR-Sudoku* dataset, which combines challenging visual perception and symbolic reasoning.

2 Related Work

Unsupervised visual concept learning is concerned with obtaining concept-level representations from unlabeled images [19]. Where some works have tackled this only for specific domains, *e.g.*, to extract “teachable” concepts for chess [53] or manipulation concepts via videos of task demonstrations [32] others depend on object-level concept guidance from initial image segmentations [21] or “natural supervision” [41]. In contrast, Vedantam et al. [68] and Wüst et al. [71] consider learning higher-level, relational concepts, *i.e.*, assuming basic-level concepts have been provided. Related to their task-supervised manner of learning concepts, Wang et al. [69] obtain concepts via the training signal from their image classification task, thereby focusing on image-region-based concepts. Recently, several works have also investigated the potential of leveraging the knowledge stored in large pretrained models, *e.g.*, via combinations of large-language models and CLIP embeddings [72, 43] or weakly-supervised queries to a vision-language model [4]. These works contain some form of supervision via text, class labels, or on the prompt level. In contrast, in this work we learn unsupervised concepts on both object and factor levels, which remain inherently inspectable and revisable.

The motivation for **inherently inspectable and revisable concept representations** is to allow human stakeholders to investigate and potentially revise a model’s internal concepts. A majority of research focuses on post-hoc approaches based on distilling concept knowledge from pretrained models [73, 16, 74, 48, 13, 17]. In contrast, Lage and Doshi-Velez [29] investigate how to learn inspectable concept representations via human feedback, focusing hereby on tabular data and higher-level concepts. Additionally, Stammer et al. [60] learn inherently inspectable visual concepts via weak supervision and a prototype-based binding mechanism. No single work develops inherently inspectable and revisable concept representations in the context of unsupervised visual learning.

The different properties of **discrete vs. continuous encodings** is a vibrant research topic that is very relevant for learning suitable concept representations. Continuous encodings allow for easier and more flexible optimization and information binding [36, 55, 56, 3]. Discrete representations are, however, considered to be vital for understanding AI models [25] and for mitigating shortcut learning [59], but also beneficial for solving complex visual reasoning tasks [20, 57]. However, learning discrete representations via neural modules is a challenging problem [37, 18, 15, 65]. Where some works have focused on categorical-distribution-based discretization [2, 22, 39], others have investigated the potential of retrieval-based discretization of continuous encodings via different forms of inherent “codebooks” [64, 62]. Only a few have investigated how to *explicitly* bind semantic visual information to specific discrete representations [60]. Where previous works mainly focus on one of

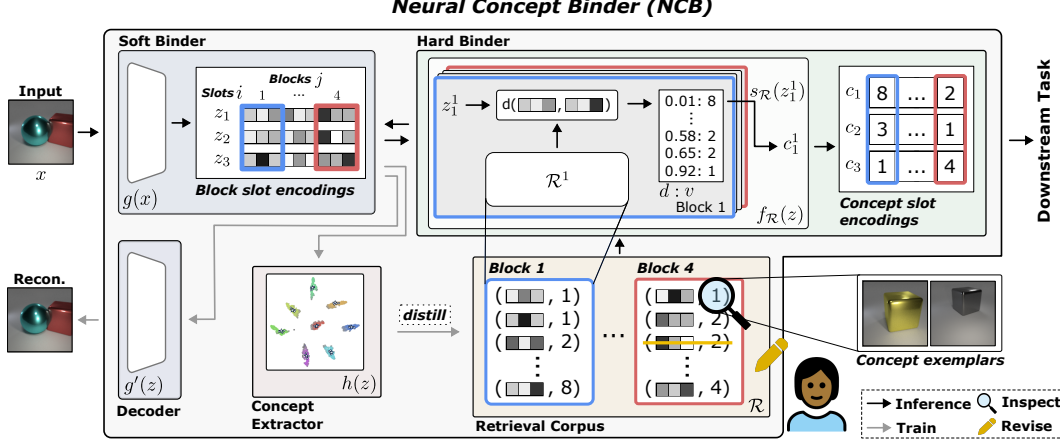


Figure 2: The **Neural Concept Binder (NCB)** combines (i) continuous, block-slot encodings via slot-attention based image processing with (ii) discrete, concept-slot encodings via retrieval-based inference. The retrieval corpus (distilled from the block-slot encodings) allows for easy concept inspection and revision by human stakeholders. Moreover, the resulting concept-slot encodings can be easily integrated into complex downstream tasks.

the two representation types, we see great potential in the recent trend of explicitly integrating both types of representations [12].

3 Neural Concept Binder (NCB): Extracting Hard from Soft Concepts

Our proposed Neural Concept Binder (NCB) framework tackles the challenge of learning inspectable and revisable object-factor level concepts from unlabeled images by combining two key elements: (i) continuous representations via (block-)slot-attention [36] based image processing with (ii) discrete representations via retrieval-based inference. Fig. 2 provides an overview of NCB’s inference, training, concept inspection, and revision processes. Let us now formally introduce these processes.

In this work, we refer to a concept as "the label of a set of things that have something in common" [1]. This definition can be applied on different scales of a visual scene: on an image level (e.g., an image of a *park*), an object level (e.g., a *tree* vs. a *bird*) or an object-factor level (e.g., the *color* of a bird). Overall, we consider a set of *unlabeled* images $X := (x_1, \dots, x_N) \in \mathbb{R}^{N \times D}$ with $x_i \in \mathbb{R}^D$, $N \in \mathbb{N}$ and $D \in \mathbb{N}$ (for simplicity, we drop the image index notation in the following). Briefly, given an image x , NCB derives a symbolic representation, c , which expresses the concepts of the objects in the image, i.e., object-factor level concepts. Herefore, NCB infers a block-slot encoding, z , of the image and performs a retrieval-based discretization step to finally infer *concept-slot encodings*, c . We begin by introducing the inference procedure of NCB. We hereby assume that NCB’s components have already been trained and will introduce details of the training procedure subsequently.

3.1 Inferring Concept-Slot Representations

Obtaining Continuous Block-Slot-Encodings. Consider an image $x \in X$. The first component of NCB, the *soft binder*, is represented via a block-slot encoder, $g_\theta : x \rightarrow z \in \mathbb{R}^{N_S \times N_B \times D_B}$, where g is parameterized by θ (unless required, this notation is omitted in the following). The soft binder transforms an input image into a latent, continuous *block-slot* representation, where N_S represents the number of slots, N_B the number of blocks per slot, and D_B the dimension of a block. It hereby utilizes two important types of *binding* mechanisms: spatial and factor binding. Spatial binding ensures spatial modularity across the entire scene and is achieved via slot attention [36]. As a result, each object in the image is represented in a specific slot, z_i , for slot i . Factor binding, on the other hand, as introduced by [56] ensures that different object *factors* (e.g., object attributes like color) are separately encoded in different blocks of a slot encoding, i.e., z_i^j for block j . These two binding mechanisms jointly perform valuable object- and factor-based image processing. Overall,

the resulting block-slot encodings represent continuous object-centric encodings of an input image (cf. Fig. 2), with objects encoded in slots and object factors encoded in blocks within the slots.

Obtaining Discrete Concept-Slot-Encodings. The role of NCB’s second processing component, the *hard binder*, is to transform these continuous block-slot encodings into expressive, yet *discrete* concept-slot encodings. Specifically, the hard binder is represented via a retrieval encoder, f , (cf. Fig. 2). It processes the block-slot encodings, z , into a set of discrete concept-slot encodings, c . We refer to its underlying binding mechanism as *concept binding*. In detail, f represents a function $f_{\mathcal{R}} : z \rightarrow c \in \mathbb{N}^{N_S \times N_B}$ that is parameterized by a retrieval corpus \mathcal{R} . This retrieval corpus consists of a tuple of sets $\mathcal{R} := [\mathcal{R}^1, \dots, \mathcal{R}^{N_B}]$ where, in turn, each $\mathcal{R}^j := \{(\text{enc}_l^j, v_l) : l \in \{1, \dots, |\mathcal{R}^j|\}\}$ contains tuples of encodings, $\text{enc}_l^j \in \mathbb{R}^{D_B}$, and corresponding discrete values, $v_l \in \{1, \dots, N_C\}$. Importantly, enc_l^j consists of a representative block encoding of a specific *concept*. Such a concept is determined in NCB’s training phase and represents a distinct group of similar block representations (cf. Fig. 2, formal details below). The value v_l thus represents the *symbol* identifier that corresponds to the specific concept that enc_l^j is associated with. Hereby, each block contains up to $N_C \in \mathbb{N}$ different concepts. To infer the concept symbol of a sample’s block-slot encoding, NCB compares z_i^j to the encodings in the corresponding block’s retrieval corpus, \mathcal{R}^j , and selects the most likely concept. Specifically, given a distance metric $d(\cdot, \cdot)$ and the block-slot encoding, z_i^j , the selection function $s_{\mathcal{R}} : z_i^j \rightarrow l \in \mathbb{N}$ finds the index l of the closest encoding in the retrieval corpus: $s_{\mathcal{R}}(z_i^j) = \text{argmin}_l d(\text{enc}_l^j, z_i^j)$ such that $(\text{enc}_l^j, v_l) \in \mathcal{R}^j$. This results in the concept representation for slot i and block j denoted as $c_i^j := v_{s_{\mathcal{R}}(z_i^j)}$. For the slot i , we thus obtain $c_i := [c_i^1, \dots, c_i^{N_B}]$. The final concept-slot encoding is given by $c := f_{\mathcal{R}}(z) = [c_1, \dots, c_{N_S}]$. We further refer to Suppl. A.1 for details on an alternative, *top-k* selection function. Let us now move on to NCB’s training procedure.

3.2 Unsupervised Concept Learning via NCB

The training procedure of the Neural Concept Binder is separated into two subsequent steps where we provide an overview here and details in Suppl. A.2. We formally describe these steps using the pseudo-code in Alg. 1. The first step consists of optimizing the encoder, g , to provide *object-factorised* block-slot encodings. It is optimized for unsupervised image reconstruction based on the decoder model, $g'_{\theta'} : z \rightarrow \tilde{x} \in \mathbb{R}^D$ (cf. Fig. 2) and utilising a mean squared error loss: $L = L_{\text{MSE}}(x, g'(g(x)))$. The goal of NCB’s second training step is to obtain the retrieval corpus, \mathcal{R} . This procedure is based on obtaining an optimal clustering of block encodings via an unsupervised clustering model, h , and distilling the resulting information from h into explicit representations in the retrieval corpus. Thus, for each block j a clustering model h_{ϕ^j} (cf. Fig. 2) is fit to identify a (potentially overparameterised) optimal set of clusters within a set of block encodings. This is based on an unsupervised criteria, e.g., a density-based score [44], and results in $N_C \in \mathbb{N}$ clusters. Next, for each cluster, $v \in \{1, \dots, N_C\}$, representative block encodings, enc^j , are extracted from h . Such an encoding represents either an averaged *prototype* or instance-based *exemplar* encoding. The corresponding tuples (enc^j, v) are explicitly stored in the retrieval corpus \mathcal{R}^j , and the final retrieval corpus consists of the set of individual corpora for each block, $\mathcal{R} = [\mathcal{R}^1, \dots, \mathcal{R}^{N_B}]$. Through this training procedure, NCB learns to unsupervisedly categorize the object-factor information from the latent encoding space of the soft binder and stores this information in a structured, symbolic, and accessible way in the hard binder’s retrieval corpus. We refer to the resulting clusters of each block as NCB’s *concepts*. In the following we denote concepts with a capital letter for the block and a natural number for the category id, e.g., $A3$. We note that in practice, it is further possible to finetune the block-slot encoder, g , through supervision from the hard binder (cf. Fig. 2), e.g., once initial categories have been identified, and can be achieved via a standard supervised approach. Ultimately, this allows for *dynamically* finetuning NCB’s concept representations. Let us now introduce how human stakeholders can inspect and revise NCB’s learned concepts.

3.3 Inspecting NCB’s Concepts

One key advantage of NCB’s concept representations is their inherent readability and inspectability. Specifically, NCB inherently enables: (i) *implicit*, (ii) *comparative*, (iii) *interventional* and (iv) *similarity*-based inspection (cf. Fig. 3). Where the first three aim at investigating NCB’s explicit,

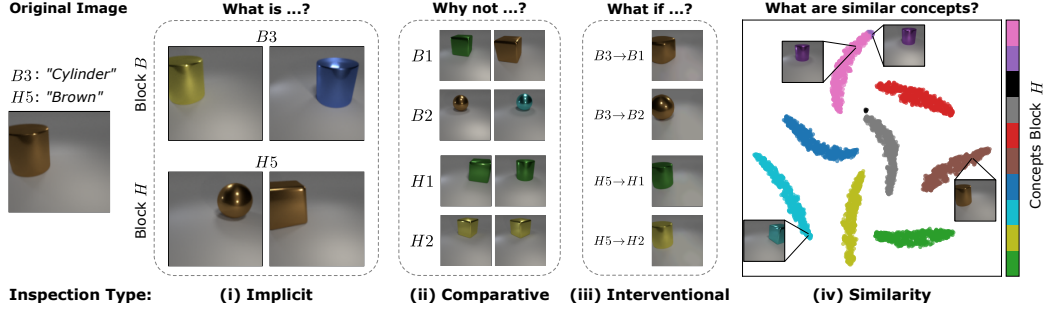


Figure 3: **NCB’s concept space is inherently inspectable.** A human stakeholder can easily inspect the concept space by asking a diverse set of questions. For example, NCB answers interventional questions (iii) via generating images with selectively modified concepts.

symbolic concept space (stored in \mathcal{R}), the last one aims at investigating its latent, continuous concept space (stored in θ).

(i) Implicit inspection queries the model to provide a set of examples for a specific concept. Essentially, this answers the question *"What are examples of this concept?"*. NCB answers this question in two ways: by providing samples from the retrieval corpus corresponding to *exemplars* of the concept or by identifying additional data samples belonging to the concept at hand.

(ii) Comparative inspection, on the other hand, allows comparing two specifically different concepts, *e.g.*, *"Why does this object depict concept H5 and not concept H1?"*. NCB hereby provides examples for both concepts for the user to compare and potentially identify dissimilar properties. Ultimately, this form of inspection allows to answer questions of the form *"Why not ...?"* and represents a valuable tool for in-depth and targeted concept inspection.

(iii) Interventional inspection allows to answer questions such as *"What if this object would have concept H1?"* To answer this question, NCB utilizes its decoder g' . Specifically, by swapping the block z_i^j of a data sample’s block-slot encoding with that of a representative sample, $(\text{enc}_l^j, v_l) \in \mathcal{R}^j$, NCB can provide an *interventional* image reconstruction, from which the effect of the swapped concept can be observed. Ultimately, this form of inspection allows to answer important questions of the form *"What if ...?"*.

Finally, **(iv) Similarity inspection** allows inspecting NCB’s *continuous* encoding space on a more global level (in comparison to the more symbolic, sample-based inspection above), *e.g.*, *"What are similar concepts to this concept?"*. Specifically, NCB’s distance metric d directly provides information about the similarity between concepts in the continuous representation. Inspecting the block-slot encoding space thus allows to identify a suboptimal soft binding, *e.g.*, when block encodings are similar according to g but not according to the human stakeholder. Overall, these inspection mechanisms allow a human stakeholder to ask a diverse set of questions concerning a model’s learned concepts.

3.4 Revising NCB’s Concepts

Let us now describe how a human stakeholder can revise NCB’s concept space. Below, we provide details on the three main actions for *symbolic* revision (*i.e.*, revision on the representations in \mathcal{R}): (i) merging, (ii) deleting, or (iii) adding information. These actions can be performed on a single encoding or on a concept level and essentially represent a form of "reorganization" of information stored in \mathcal{R} . Furthermore, we provide details on how to (iv) revise the continuous latent space, which essentially requires finetuning of g ’s parameters.

(i) Merge Concepts: In the case that \mathcal{R} contains multiple concepts that, according to human knowledge, represent a joint underlying concept (*e.g.*, two concepts for purple in Fig. 3 (right)) it is easy to update the model’s internal representations by replacing the concept symbols of one concept with those of the second concept. Formally, (in the case of two concepts) if v_l and v_m of block j should be *merged*, the information stored in \mathcal{R}^j is updated via $\forall(\text{enc}_l^j, v_l) : v_l \rightarrow v_m$.

Table 1: **Comparison of different approaches for concept learning.** Hereby, we differentiate based on the following categories: whether a method (1) is learned in an unsupervised fashion, (2) provides object-level concepts (*i.e.*, can explicitly process multiple objects), (3) provides factor-level concepts (*i.e.*, the color green), (4) provides continuous concept encodings, (5) provides discrete concept encodings, (6) provides inherently inspectable and (7) revisable concept representations.

Method	Unsupervised	Obj. level	Factor level	Cont. encs	Disc. encs	Inspectable	Revisable
CBM [28]	✗	✗	✓	✗	✓	✓	✓
NeSyCL [59]	✗	✓	✓	✗	✓	✓	✓
GlanceNets [42]	✗	✗	✓	✓	✓	✓	✓
VAE [27]	✓	✗	✗	✓	✗	✗	✗
VQ-VAE [66]	✓	✗	✗	✓	✓	✗	✗
SA [36]	✓	✓	✗	✓	✗	(✓)	✗
SysBinder [56]	✓	✓	✓	✓	✗	(✓)	✗
Neural Concept Binder	✓	✓	✓	✓	✓	✓	✓

(ii) Delete Encodings or Concepts: If \mathcal{R} contains an encoding for a specific concept that does not match the other encodings of that concept, *e.g.*, a misplaced exemplar, this encoding can simply be removed via $\text{remove}((\text{enc}_l^j, v_l))$. Accordingly, if an entire concept is identified as suboptimal, it is possible to delete all corresponding encodings of concept m in \mathcal{R}^j as $\forall(\text{enc}_l^j, v_l) : v_l = m \implies \text{remove}((\text{enc}_l^j, v_l))$.

(iii) Add Encodings or Concepts: In a similar fashion, it is also possible to add encodings to \mathcal{R} . For instance, if a specific concept is not sufficiently well captured via the encodings in \mathcal{R}^j , one can add an additional encoding, enc_l^j , for the concept, m , via $\text{add}((\text{enc}_l^j, m))$. Accordingly, it is also possible to add encodings for an entire concept, $\hat{v}_l : \forall(\text{enc}_l^j, \hat{v}_l) \implies \text{add}((\text{enc}_l^j, m))$

(iv) Revise the (Continuous) Latent Space: Lastly, if the soft binder provides suboptimal object- and factor-level block-slot encodings, it is further possible to integrate revisory feedback on the soft binder’s continuous latent space. This can be achieved via additional finetuning of the soft binder’s parameters, θ , *e.g.*, via standard forms of weak supervision [35, 60] or interactive learning [59, 52].

In summary, our novel Neural Concept Binder framework fulfills several important desiderata for concept learning (*cf.* Tab. 1). Specifically, NCB learns concepts in an unsupervised fashion that are structured on both an object (*i.e.*, can explicitly process multiple objects) and factor-level. Furthermore, next to standard continuous encodings, NCB also provides discrete concept representations, which are crucial for interpretability and integration into symbolic computations. Lastly, NCB’s concept space is inspectable and revisable, essential for unsupervised learned concept representations.

4 Experimental Evaluations

In our evaluations, we investigate the potential of NCB’s soft and hard binding mechanisms in unsupervised concept learning and its integration into downstream tasks. Notably, NCB encompasses concept processing between both of its components (soft binder and hard binder) whereby the direction "soft binder \leftarrow hard binder" (*cf.* Fig. 2) represents a standard approach (*i.e.*, supervised learning of the soft binder’s encoding space via symbolic concept labels, *e.g.*, [28, 59]). Therefore, we focus our evaluations on NCB’s more novel processing direction, "soft binder \rightarrow hard binder". We aim to answer the following research questions: **(Q1)** Does NCB provide **expressive** and **distinct** encodings? **(Q2)** Can NCB be combined with **symbolic** methods to solve complex downstream tasks? **(Q3)** Can NCB’s learned concepts be **revised** to improve suboptimal behaviour? **(Q4)** Can NCB be combined with **subsymbolic** methods to *transparently* solve complex downstream tasks?

Data. We focus our evaluations on different variations of the popular CLEVR dataset. Specifically, we investigate (Q1 & Q3) in the context of the CLEVR [24] and CLEVR-Easy [56] datasets. For investigating the integration of NCB into symbolic modules (Q2), we utilize our novel CLEVR-Sudoku puzzles introduced in the following. Finally, to evaluate the integration of NCB into subsymbolic modules (Q4), we evaluate on confounded and non-confounded variants of the CLEVR-Hans3 dataset [59]. We provide further details on these datasets in the supplements (*cf.* Suppl. C).

CLEVR-Sudoku. To investigate the potential of integrating NCB’s discrete concept representations into symbolic downstream tasks, we introduce the novel CLEVR-Sudoku dataset. It represents a challenging visual puzzle requiring both visual object perception and reasoning capabilities. Each sample of the dataset (*cf.* Fig. 4 for an example puzzle) consists of a Sudoku puzzle that is (partially filled) with CLEVR-based images [24] and additional example images that depict the mapping of relevant object properties to digits. Specifically, each digit of the Sudoku is replaced by an image of an object. All objects representing the same digit share a set of common properties, *e.g.*, in Fig. 4 all objects replacing "1"s are yellow spheres. We introduce two variants of CLEVR-Sudoku: *Sudoku CLEVR-Easy* and *Sudoku CLEVR*. In the first one, all objects are large and metallic, leaving only shape and color as properties for the digits. In *Sudoku CLEVR*, the size and material of the CLEVR objects are also relevant for the digits. Moreover, up to 10 example images are provided per digit mapping; the fewer examples provided, the harder it is to learn the mapping. The initial state and digit-attribute mapping vary for each sample. One specific intricacy of CLEVR-Sudoku is that a Sudoku can only be solved if all subcell images are correctly mapped to the digits. Even one mistake can lead to an unsolvable Sudoku. Thus, in comparison to standard Sudoku puzzles, which mainly require deductive reasoning, solving CLEVR-Sudoku additionally requires complex object recognition and the ability to map these visual concept perceptions to the *task concepts* (*i.e.* the 9 digits of Sudoku). We refer to Suppl. B for further details.

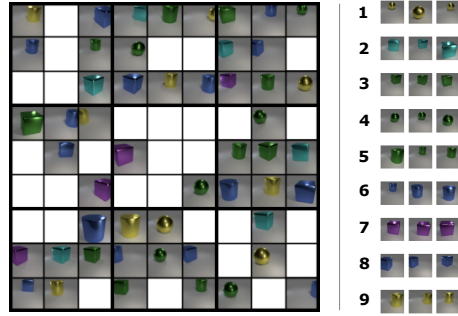


Figure 4: **Example from CLEVR-Sudoku.** Each digit is represented by CLEVR objects with the same attribute combination. The objective is to solve the Sudoku only based on the initial grid of CLEVR images and the digit mapping of candidate examples.

Models. For our evaluations, we instantiate Neural Concept Binder based on the SysBinder model [56] for the soft binder encoder, g , and hdbscan [8, 9] for the clustering model, h . We refer to Suppl. A.3 for all additional details. In the context of (Q1), we compare NCB’s results to those of four different variations of the SysBinder model [56]. We denote the original SysBinder configuration as *SysBinder (cont.)* (provides continuous block-slot encodings). For *SysBinder*, we discretize SysBinder’s continuous encodings at inference time (via an argmin operation over SysBinder’s internal codebooks). *SysBinder (hard)* is trained from the start to provide discrete encodings (via a low codebook softmax temperature). *SysBinder (step)* is trained by step-wise decreasing this temperature (*cf.* Suppl. D for details). For evaluations on CLEVR-Sudoku (Q2+Q3), we first infer NCB’s discrete concept-slot encodings for a puzzle’s candidate examples. These encodings (together with the corresponding digit labels) are passed to a symbolic classifier, which is fit to predict the digits from the encodings. Next, this classifier infers the digits from the image of each subcell in the puzzle’s initial state. These are used by a constraint propagation and search-based algorithm [46, 6] to solve the puzzle (*cf.* Suppl. E.2 for details). We denote the combination of the symbolic classifier and constraint solver as *solver*. We compare the solver’s performance when provided ground-truth (GT) object-property labels (*GT concepts*), encodings from a supervised trained slot attention encoder [36] (*SA (supervised)*) and the discrete encodings from *SysBinder* (denoted here as *SysBinder (unsupervised)*). For classification evaluations (Q4), we evaluate a configuration in which a set transformer classifier [31] is provided NCB’s concept encodings (*NCB + NN*) and makes a final class prediction based on these (*cf.* Suppl. E.4). We compare to *SA + NN*, *i.e.*, where a supervised trained slot attention encoder [36] provides object-property predictions.

Metrics. We evaluate all models based on their accuracies on held-out test splits, each with 3 seeded reruns. We provide average accuracies and standard deviations over these. When assessing the expressiveness of NCB’s concept-slot encodings (Q1), we evaluate the accuracy for object-property prediction. When evaluating the performance of the downstream tasks, we provide the percentage of solved CLEVR-Sudokus (Q2) and the classification accuracy on the test set of CLEVR-Hans3 (Q4).

4.1 Evaluations

Discrete, yet expressive representations (Q1). In (Q1), we investigate how much valuable information NCB’s discrete concept-slot encodings contain, despite NCB’s inherent information bottleneck.

Table 2: **NCB’s concept encodings are expressive despite information bottleneck.** Classifying object properties from different continuous and discrete encodings. The classifier is provided with different amounts of training sample encodings. The best (“•”) and runner-up (“◦”) results are bold.

Dataset	N Train	SysBinder (cont.)	SysBinder	SysBinder (hard)	SysBinder (step)	Neural Concept Binder
CLEVR-Easy	N=2000	• 99.83 ±0.24	92.49±5.45	22.92±0.00	95.76±4.92	◦ 99.02 ±1.00
	N=200	• 99.20 ±0.41	87.90±8.05	22.92±0.00	92.42±7.32	◦ 98.50 ±1.80
	N=50	◦ 91.13 ±4.21	78.41±8.69	22.92±0.00	70.64±11.89	• 95.87 ±2.93
	N=20	◦ 64.88 ±10.89	62.61±7.18	22.92±0.00	54.61±9.57	• 94.22 ±4.11
CLEVR	N=2000	• 98.86 ±1.15	86.22±10.40	36.46±0.00	88.90±14.81	◦ 97.26 ±2.67
	N=200	• 97.61 ±2.58	81.13±12.39	36.46±0.00	83.17±17.05	◦ 96.80 ±3.01
	N=50	◦ 93.25 ±4.62	61.67±8.51	36.46±0.00	68.81±17.74	• 94.67 ±4.65
	N=20	◦ 79.11 ±8.75	49.79±6.73	36.46±0.00	58.58±16.09	• 88.57 ±4.68

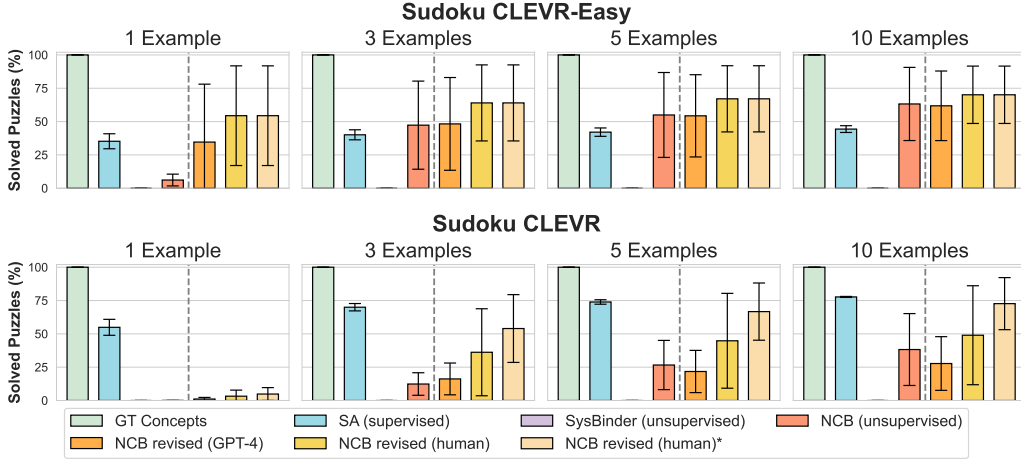


Figure 5: **NCB’s unsupervised concepts allow solving symbolic puzzles.** Accuracy of solved Sudokus via different discrete concept encodings on Sudoku CLEVR-Easy and Sudoku CLEVR (left sides). Additional revision on NCB’s concepts leads to improved performances (right sides).

For this purpose, we train a classifier on NCB’s encodings to predict corresponding object-property labels, *e.g.*, the color green (*cf.* Suppl. E.1 for details). In Tab. 2 we provide results for the CLEVR-Easy and CLEVR dataset with a classification training set of 2000, 200, 50, or 20 encodings. Focusing first on the results for $N = 2000$, we observe that, as expected, the continuous representation of the original Sysbinder model contains the most information compared to all discrete encodings. Remarkably, however, NCB’s discrete concept representations are nearly on par with the continuous encodings. This is particularly remarkable given the immense information bottleneck in NCB². Moreover, we observe that NCB’s encodings greatly outperform all other forms of discrete representations. Focusing now on the results when the classifier is trained on data subsets, we observe a substantial degradation in performance via encodings of any of the discrete baselines, and the continuous encodings. In stark contrast, when classifying based on NCB’s encodings, the accuracy remains nearly constant even with 1% of the initial training samples. We provide additional ablations on the effect of concept encoding types and NCB’s selection function in Suppl. F.1 as well as an ablation analysis on the effect of suboptimal behavior from NCB’s individual components in Suppl. F.2. We further refer to Suppl. F.3 for an analysis of NCB’s obtained concept space as well as Suppl. G for examples of learned concepts. Overall, our results provide evidence for the expressiveness of NCB’s concept encodings despite their enormous information bottleneck. Furthermore, our results for $N \leq 200$ suggest that the information stored in the NCB’s encodings is easier to generalize compared to the baselines. We thus answer **Q1** affirmatively.

Utilising unsupervised concepts for solving visual Sudoku (Q2). In our following evaluations, we investigate the potential of NCB’s representations for solving complex reasoning tasks via their integration into symbolic computations. We base these evaluations on our novel CLEVR-Sudoku

²SysBinder (cont.) provides 2048-sized continuous encodings, whereas NCB provides discrete encodings of size ≤ 16 .

Table 3: **NCB’s unsupervised concept representations facilitate interpretable neural computations.** Explanations of a NN classifier trained on the unsupervised concepts of NCB. Via NCB’s inherent inspection procedures a human stakeholder can identify which concepts the classifier focuses on to make its predictions and thus interpret the NN’s underlying decision rule.

GT Class Rule	NN Expl.	Human Inspection	Human Interpretation
Large, gray cube	$C3 \wedge H4 \wedge K4$ $\wedge O12 \wedge P5$	$(\text{Gray1}) \wedge (\text{Red} \vee \text{Gray2}) \wedge (\text{Large}) \wedge$ $(\text{Gray3}) \wedge (\text{Gray4})$	“A large gray object”
Small, metal cube	$B3 \wedge D3 \wedge H0$ $\wedge I0 \wedge K0$	$(\text{Cube}) \wedge (\text{Small1}) \wedge (\text{Small2}) \wedge (\text{Small3})$ $\wedge (\text{Small4})$	“A small cube”
Large, blue sphere	$B0 \wedge C6 \wedge H3$ $\wedge O0 \wedge P1$	$(\text{Sphere}) \wedge (\text{Blue1}) \wedge (\text{Blue2}) \wedge (\text{Small} \vee$ $\text{Blue3}) \wedge (\text{Blue4} \vee \text{Green} \vee \text{Purple})$	“A blue sphere”

dataset. We report the percentage of solved puzzles for CLEVR-Sudoku in Fig. 5. Hereby, it is important to note that the solver can only solve a puzzle if each of the images of the initial state has been classified correctly. Thus, the results of Fig. 5 represent “all-or-nothing” results. Focusing on the results left of the dashed lines, we observe that the symbolic module can solve every puzzle with GT concepts, even when only one example image is provided. Interestingly, performance drops drastically when provided with encodings of *SA* (*supervised*). This highlights the difficulty of the CLEVR-Sudoku puzzles: minor errors in digit prediction can lead to major errors in solving the underlying puzzle. When comparing the performance via encodings from the two unsupervised models, we observe quite strong performances via NCB’s concept encodings. *e.g.*, they allow to solve $\approx 50\%$ for the 10 example configurations (over both data settings) in comparison to $\approx 61\%$ for *SA* (*supervised*). In contrast, when provided *SysBinder*’s encodings the solver fails over all Sudoku variations. This demonstrates the effectiveness of NCB’s binding mechanisms over solely those of the *SysBinder* approach. We refer to Suppl. F.4 for further discussions as well as quantitative digit classification results. Overall, our evaluations highlight the potential of NCB’s unsupervised concept encodings for solving complex, symbolic downstream tasks. We therefore answer **Q2** affirmatively.

Easily revising NCB’s concepts (Q3). In our next evaluations, we illustrate the potential of NCB’s revision procedures. As revision on the continuous latent space of NCB’s soft binder is analogous to existing approaches (*e.g.*, [52, 49, 60]), we focus these evaluations on the novel, NCB-specific forms of *symbolic* revision, *i.e.*, on the hard binder’s concept space. We hereby illustrate the first two forms of symbolic revision (*removing* and *merging* concept information) via two forms of feedback: based on a pretrained vision-language model (here via GPT-4 [47]) and simulated human feedback. In both cases, we ask the revisory agent to identify which concepts in each block should be removed or merged based on exemplar images of each concept, *i.e.*, implicit concept inspection (*cf.* Suppl. E.3 for details). In Fig. 5 we provide CLEVR-Sudoku performances when the NCB’s retrieval corpus has been updated based on the different revisory agents (*i.e.*, *NCB revised (GPT-4)* and *NCB revised (human)*). Interestingly, although we observe improvements in the few example settings via GPT-4’s revisions, we observe a negative effect in the settings with more digit examples. This is due to the suboptimal behavior of GPT-4 in providing consistent object descriptions, such that too much concept information is removed or merged and highlights the effect of “ill-informed” feedback (*cf.* Suppl. F.5). In contrast, when provided with human revision, we observe a substantial boost in Sudoku performance, particularly in puzzle configurations with few candidate examples. Moreover, via NCB’s similarity inspection mechanism (*cf.* Sec. 3.3), a human stakeholder can easily identify models that provide suboptimal soft binding processing. In this case, such models can be excluded from further downstream evaluations (*cf.* *NCB revised (human)**) and must be refined via finetuning *g*’s parameters (*e.g.*, via approaches of [52, 49, 60]). In Suppl. F.6, we further investigate concept revision via *adding* information. Overall, our results highlight the potential and ease of revising NCB’s concept space. We thus answer **Q3** positively.

Utilising unsupervised concepts for understanding neural computations (Q4). In our final evaluations, we investigate whether NCB’s concept encodings can make *subsymbolic* computations more transparent. Therefore, we consider the task of image classification on variations of the benchmark CLEVR-Hans3 dataset [59]. While the concept encodings in *NCB + NN* are trained *unsupervised*, they perform on par with those of the supervised approach of [59] (*cf.* Suppl. F.7). Even more important, integrating NCB’s inherently inspectable concept representations into neural computations can elicit more transparent decision processes. We illustrate this in Tab. 3, where we exemplify class-level

explanations of the classifier of *NCB + NN* (cf. Suppl. E.4 for details). Via NCB’s inspection mechanisms, a human stakeholder can now easily identify the classifier’s internal decision rule for a class (e.g., "a large gray object"). Overall, this is a vital feature for the deployment of trustworthy AI models in real-world scenarios and the significance of our results is, that we can achieve this even when utilising *unsupervised* concept encodings. Moreover, in Fig. 6 we investigate whether a NCB-based neural classifier can be revised to mitigate the confounders in CLEVR-Hans3 (cf. Suppl. E.4 and Suppl. F.8 for details). The confounding factor in the training set is the color *gray*. We present the non-confounded test set accuracy in Fig. 6. We observe that standard loss-based feedback via explanatory interactive learning (XIL) [59] on the NN classifier’s explanations (+ *XIL on NN*) can greatly reduce the effect of the confounder. Alternatively, by simply zeroing the activations of the undesired concept *gray* (+ *XIL on concepts*) we even achieve improved confounding mitigation results without the usual issues of joint optimization. Overall, our results highlight the potential of integrating NCB’s unsupervised concept representations for eliciting transparent and trustworthy subsymbolic computations. We thus answer **Q4** affirmatively.

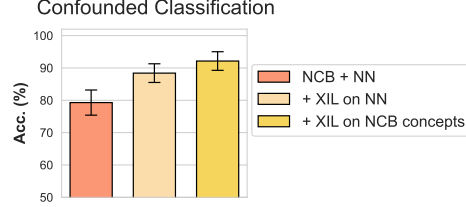


Figure 6: **NCB’s unsupervised concept representations facilitate shortcut mitigation.** Test accuracy for classification via NN predictor when trained on *confounded* images.

Limitations. NCB largely benefits from qualitative initial block-slot encodings. If these are lacking, the extracted concept-slot encodings lose quality as well. An important next step to handle more complex visual inputs, e.g., video data, is the integration of recent approaches, e.g., [11, 14]. Furthermore, due to the unsupervised nature of NCB’s training, additional alignment of NCB’s concepts is inevitable for deployment in downstream tasks [5]. Further, to build trust in NCB’s concept knowledge, human inspection is required. Lastly, revisions are an integral part of NCB. However they rely on humans to provide "good" feedback, as a malicious user can manipulate NCB’s concepts. However, inspecting the concept space allows to track this effectively.

5 Conclusions

In this work, we introduce the Neural Concept Binder framework for learning visual object-factor concepts in an unsupervised fashion. Our evaluations suggest that NCB’s specific binding mechanisms benefit learning expressive yet discrete concept representations. Moreover, our evaluations highlight the potential of integrating NCB’s inherently inspectable and revisable concept-slot encodings into symbolic *and* neural modules. Interesting avenues for future research are investigating the benefits of NCB’s concept representations in the context of continual learning settings [7] as well as integrating NCB’s basic level concepts into high-level concept learning approaches [71], but also probabilistic logic programming approaches [57, 58]. Additionally, integrating learning signals from a downstream task into NCB’s concept representations, e.g., via differentiable clustering [67], is important for improving the quality of initial concept encodings.

Acknowledgments

The authors wish to thank Gautam Singh for initial help with SysBinder. Furthermore, the authors wish to thank Cyprien Dzialo for his preliminary results and insights on this project. This work was supported by the Priority Program (SPP) 2422 in the subproject "Optimization of active surface design of high-speed progressive tools using machine and deep learning algorithms" funded by the German Research Foundation (DFG), the "ML2MT" project from the Volkswagen Stiftung and the "The Adaptive Mind" project from the Hessian Ministry of Science and Arts (HMWK). It has further benefited from the HMWK projects "The Third Wave of Artificial Intelligence - 3AI", and Hessian.AI, as well as the Hessian research priority program LOEWE within the project WhiteBox, the ICT-48 Network of AI Research Excellence Center "TAILOR" (EU Horizon 2020, GA No 952215) and the EU-funded "TANGO" project (EU Horizon 2023, GA No 57100431).

References

- [1] E James Archer. The psychological nature of concepts. In *Analyses of concept learning*, pages 37–49. Elsevier, 1966.
- [2] Masataro Asai and Alex Fukunaga. Classical planning in deep latent space: Bridging the subsymbolic-symbolic boundary. In *Conference on Artificial Intelligence (AAAI)*, pages 6094–6101. AAAI Press, 2018.
- [3] Pietro Barbiero, Gabriele Ciravegna, Francesco Giannini, Mateo Espinosa Zarlenga, Lucie Charlotte Magister, Alberto Tonda, Pietro Lio, Frédéric Precioso, Mateja Jamnik, and Giuseppe Marra. Interpretable neural-symbolic concept reasoning. In *International Conference on Machine Learning (ICML)*, 2023.
- [4] Adrita Barua, Cara Widmer, and Pascal Hitzler. Concept induction using llms: a user experiment for assessment. *CoRR*, abs/2404.11875, 2024.
- [5] Aaron Bembenek and Toby Murray. Symbol correctness in deep neural networks containing symbolic layers. *CoRR*, abs/2402.03663, 2024.
- [6] Christian Bessiere. Constraint propagation. In *Foundations of Artificial Intelligence*, volume 2, pages 29–83. Elsevier, 2006.
- [7] Florian Peter Busch, Roshni Kamath, Rupert Mitchell, Wolfgang Stammer, Kristian Kersting, and Martin Mundt. Where is the truth? the risk of getting confounded in a continual world. *CoRR*, abs/2402.06434, 2024.
- [8] Ricardo J. G. B. Campello, Davoud Moulavi, and Jörg Sander. Density-based clustering based on hierarchical density estimates. In *Advances in Knowledge Discovery and Data Mining (PAKDD)*, 2013.
- [9] Ricardo J. G. B. Campello, Davoud Moulavi, Arthur Zimek, and Jörg Sander. Hierarchical density estimates for data clustering, visualization, and outlier detection. *ACM Transactions on Knowledge Discovery from Data*, 10(1):5:1–5:51, 2015.
- [10] Alex J. DeGrave, Joseph D. Janizek, and Su-In Lee. AI for radiographic COVID-19 detection selects shortcuts over signal. *Nature Machine Intelligence*, 3(7):610–619, 2021.
- [11] Quentin Delfosse, Wolfgang Stammer, Thomas Rothenbacher, Dwarak Vittal, and Kristian Kersting. Boosting object representation learning via motion and object continuity. In *European Conference on Machine Learning and Principles and Practice of Knowledge Discovery in Databases (PKDD / ECML)*, 2023.
- [12] Marius-Constantin Dinu, Claudiu Leoveanu-Condrei, Markus Holzleitner, Werner Zellinger, and Sepp Hochreiter. Symbolicai: A framework for logic-based approaches combining generative models and solvers. *CoRR*, abs/2402.00854, 2024.
- [13] Maximilian Dreyer, Reduan Achibat, Wojciech Samek, and Sebastian Lapuschkin. Understanding the (extra-)ordinary: Validating deep model decisions with prototypical concept-based explanations. *CoRR*, abs/2311.16681, 2023.
- [14] Gamaleldin F. Elsayed, Aravindh Mahendran, Sjoerd van Steenkiste, Klaus Greff, Michael C. Mozer, and Thomas Kipf. Savi++: Towards end-to-end object-centric learning from real-world videos. In *Advances in Neural Information Processing Systems (NeurIPS)*, 2022.
- [15] Jerome Feldman. The neural binding problem (s). *Cognitive neurodynamics*, 7:1–11, 2013.
- [16] Asma Ghandeharioun, Been Kim, Chun-Liang Li, Brendan Jou, Brian Eoff, and Rosalind W. Picard. DISSECT: disentangled simultaneous explanations via concept traversals. In *International Conference on Learning Representations (ICLR)*, 2022.
- [17] Shantanu Ghosh, Ke Yu, Forough Arabshahi, and Kayhan Batmanghelich. Dividing and conquering a blackbox to a mixture of interpretable models: Route, interpret, repeat. In *International Conference on Machine Learning (ICML)*, 2023.
- [18] Klaus Greff, Sjoerd van Steenkiste, and Jürgen Schmidhuber. On the binding problem in artificial neural networks. *CoRR*, abs/2012.05208, 2020.
- [19] Avani Gupta and P. J. Narayanan. A survey on concept-based approaches for model improvement. *CoRR*, abs/2403.14566, 2024.

- [20] Michael Hersche, Mustafa Zeqiri, Luca Benini, Abu Sebastian, and Abbas Rahimi. A neuro-vector-symbolic architecture for solving raven’s progressive matrices. *Nature Machine Intelligence*, 5(4):363–375, 2023.
- [21] Haiyang Huang, Zhi Chen, and Cynthia Rudin. Segdiscover: Visual concept discovery via unsupervised semantic segmentation. *CoRR*, abs/2204.10926, 2022.
- [22] Eric Jang, Shixiang Gu, and Ben Poole. Categorical reparameterization with gumbel-softmax. In *International Conference on Learning Representations (ICLR)*, 2017.
- [23] Chen Jin, Ryutaro Tanno, Amrutha Saseendran, Tom Diethe, and Philip Teare. An image is worth multiple words: Learning object level concepts using multi-concept prompt learning. *CoRR*, abs/2310.12274, 2023.
- [24] Justin Johnson, Bharath Hariharan, Laurens van der Maaten, Li Fei-Fei, C. Lawrence Zitnick, and Ross B. Girshick. CLEVR: A diagnostic dataset for compositional language and elementary visual reasoning. In *Conference on Computer Vision and Pattern Recognition (CVPR)*, 2017.
- [25] Subbarao Kambhampati, Sarath Sreedharan, Mudit Verma, Yantian Zha, and Lin Guan. Symbols as a lingua franca for bridging human-ai chasm for explainable and advisable AI systems. In *Conference on Artificial Intelligence (AAAI)*, 2022.
- [26] Eunji Kim, Dahuin Jung, Sangha Park, Siwon Kim, and Sungroh Yoon. Probabilistic concept bottleneck models. In *International Conference on Machine Learning (ICML)*, 2023.
- [27] Diederik P. Kingma and Max Welling. An introduction to variational autoencoders. *Foundations and Trends in Machine Learning*, 12(4):307–392, 2019.
- [28] Pang Wei Koh, Thao Nguyen, Yew Siang Tang, Stephen Mussmann, Emma Pierson, Been Kim, and Percy Liang. Concept bottleneck models. In *International Conference on Machine Learning (ICML)*, 2020.
- [29] Isaac Lage and Finale Doshi-Velez. Learning interpretable concept-based models with human feedback. *CoRR*, abs/2012.02898, 2020.
- [30] Thibault Laugel, Marie-Jeanne Lesot, Christophe Marsala, Xavier Renard, and Marcin Detryniecki. The dangers of post-hoc interpretability: Unjustified counterfactual explanations. In *International Joint Conference on Artificial Intelligence (IJCAI)*, 2019.
- [31] Juho Lee, Yoonho Lee, Jungtaek Kim, Adam R. Kosiorek, Seungjin Choi, and Yee Whye Teh. Set transformer: A framework for attention-based permutation-invariant neural networks. In *International Conference on Machine Learning (ICML)*, 2019.
- [32] Ruizhe Liu, Qian Luo, and Yanchao Yang. Infocon: Concept discovery with generative and discriminative informativeness. 2024.
- [33] Francesco Locatello, Stefan Bauer, Mario Lucic, Gunnar Rätsch, Sylvain Gelly, Bernhard Schölkopf, and Olivier Bachem. Challenging common assumptions in the unsupervised learning of disentangled representations. In *International Conference on Machine Learning (ICML)*, 2019.
- [34] Francesco Locatello, Ben Poole, Gunnar Rätsch, Bernhard Schölkopf, Olivier Bachem, and Michael Tschannen. Weakly-supervised disentanglement without compromises. In *International conference on machine learning (ICML)*, 2020.
- [35] Francesco Locatello, Michael Tschannen, Stefan Bauer, Gunnar Rätsch, Bernhard Schölkopf, and Olivier Bachem. Disentangling factors of variations using few labels. In *International Conference on Learning Representations (ICLR)*, 2020.
- [36] Francesco Locatello, Dirk Weissenborn, Thomas Unterthiner, Aravindh Mahendran, Georg Heigold, Jakob Uszkoreit, Alexey Dosovitskiy, and Thomas Kipf. Object-centric learning with slot attention. In *Advances in Neural Information Processing Systems (NeurIPS)*, 2020.
- [37] Luca Salvatore Lorello and Marco Lippi. The challenge of learning symbolic representations. In *International Workshop on Neural-Symbolic Learning and Reasoning*, 2023.
- [38] James MacQueen et al. Some methods for classification and analysis of multivariate observations. In *Berkeley Symposium on Mathematical Statistics and Probability*, 1967.
- [39] Chris J. Maddison, Andriy Mnih, and Yee Whye Teh. The concrete distribution: A continuous relaxation of discrete random variables. In *International Conference on Learning Representations (ICLR)*, 2017.

- [40] Anita Mahinpei, Justin Clark, Isaac Lage, Finale Doshi-Velez, and Weiwei Pan. Promises and pitfalls of black-box concept learning models. *CoRR*, abs/2106.13314, 2021.
- [41] Jiayuan Mao, Chuang Gan, Pushmeet Kohli, Joshua B Tenenbaum, and Jiajun Wu. The neuro-symbolic concept learner: Interpreting scenes, words, and sentences from natural supervision. In *International Conference on Learning Representations (ICLR)*, 2019.
- [42] Emanuele Marconato, Andrea Passerini, and Stefano Teso. Glancenets: Interpretable, leak-proof concept-based models. In *Advances in Neural Information Processing Systems (NeurIPS)*, 2022.
- [43] Mazda Moayeri, Keivan Rezaei, Maziar Sanjabi, and Soheil Feizi. Text-to-concept (and back) via cross-model alignment. In *International Conference on Machine Learning (ICML)*, 2023.
- [44] Davoud Moulavi, Pablo A. Jaskowiak, Ricardo J. G. B. Campello, Arthur Zimek, and Jörg Sander. Density-based clustering validation. In *International Conference on Data Mining*, 2014.
- [45] Frank Nielsen. Hierarchical clustering. *Introduction to HPC with MPI for Data Science*, pages 195–211, 2016.
- [46] Peter Norvig. Solving every sudoku puzzle. URL <http://norvig.com/sudoku.html>, 2006.
- [47] OpenAI. GPT-4 technical report. *CoRR*, abs/2303.08774, 2023.
- [48] Bo Pan, Zhenke Liu, Yifei Zhang, and Liang Zhao. Surrocbm: Concept bottleneck surrogate models for generative post-hoc explanation. *CoRR*, abs/2310.07698, 2023.
- [49] Andrew Slavin Ross, Michael C. Hughes, and Finale Doshi-Velez. Right for the right reasons: Training differentiable models by constraining their explanations. In *International Joint Conference on Artificial Intelligence (IJCAI)*, 2017.
- [50] Adam Santoro, Felix Hill, David G. T. Barrett, Ari S. Morcos, and Timothy P. Lillicrap. Measuring abstract reasoning in neural networks. In *Proceedings of the 35th International Conference on Machine Learning, ICML 2018, Stockholmsmässan, Stockholm, Sweden, July 10-15, 2018*, volume 80 of *Proceedings of Machine Learning Research*, pages 4477–4486. PMLR, 2018.
- [51] Yoshihide Sawada and Keigo Nakamura. Concept bottleneck model with additional unsupervised concepts. *IEEE Access*, 10:41758–41765, 2022.
- [52] Patrick Schramowski, Wolfgang Stammer, Stefano Teso, Anna Brugger, Franziska Herbert, Xiaoting Shao, Hans-Georg Luigs, Anne-Katrin Mahlein, and Kristian Kersting. Making deep neural networks right for the right scientific reasons by interacting with their explanations. *Nature Machine Intelligence*, 2(8):476–486, 2020.
- [53] Lisa Schut, Nenad Tomasev, Tom McGrath, Demis Hassabis, Ulrich Paquet, and Been Kim. Bridging the human-ai knowledge gap: Concept discovery and transfer in alphazero. *CoRR*, abs/2310.16410, 2023.
- [54] Rui Shu, Yining Chen, Abhishek Kumar, Stefano Ermon, and Ben Poole. Weakly supervised disentanglement with guarantees. In *International Conference on Learning Representations (ICLR)*, 2020.
- [55] Gautam Singh, Fei Deng, and Sungjin Ahn. Illiterate DALL-E learns to compose. In *International Conference on Learning Representations (ICLR)*, 2022.
- [56] Gautam Singh, Yeongbin Kim, and Sungjin Ahn. Neural systematic binder. In *International Conference on Learning Representations (ICLR)*, 2023.
- [57] Arseny Skryagin, Wolfgang Stammer, Daniel Ochs, Devendra Singh Dhami, and Kristian Kersting. Neural-probabilistic answer set programming. In *International Conference on Principles of Knowledge Representation and Reasoning (KR)*, 2022.
- [58] Arseny Skryagin, Daniel Ochs, Devendra Singh Dhami, and Kristian Kersting. Scalable neural-probabilistic answer set programming. *Journal of Artificial Intelligence Research*, 78:579–617, 2023.
- [59] Wolfgang Stammer, Patrick Schramowski, and Kristian Kersting. Right for the right concept: Revising neuro-symbolic concepts by interacting with their explanations. In *Conference on Computer Vision and Pattern Recognition (CVPR)*, 2021.

- [60] Wolfgang Stammer, Marius Memmel, Patrick Schramowski, and Kristian Kersting. Interactive disentanglement: Learning concepts by interacting with their prototype representations. In *Conference on Computer Vision and Pattern Recognition (CVPR)*, 2022.
- [61] Mukund Sundararajan, Ankur Taly, and Qiqi Yan. Axiomatic attribution for deep networks. In *International Conference on Machine Learning (ICML)*, 2017.
- [62] Alex Tamkin, Mohammad Tafseeque, and Noah D. Goodman. Codebook features: Sparse and discrete interpretability for neural networks. *CoRR*, abs/2310.17230, 2023.
- [63] Sever Topan, David Rolnick, and Xujie Si. Techniques for symbol grounding with satnet. In *Advances in Neural Information Processing Systems (NeurIPS)*, 2021.
- [64] Frederik Träuble, Anirudh Goyal, Nasim Rahaman, Michael Curtis Mozer, Kenji Kawaguchi, Yoshua Bengio, and Bernhard Schölkopf. Discrete key-value bottleneck. In *International Conference on Machine Learning (ICML)*, 2023.
- [65] Anne Treisman. Solutions to the binding problem: progress through controversy and convergence. *Neuron*, 24(1):105–125, 1999.
- [66] Aäron van den Oord, Oriol Vinyals, and Koray Kavukcuoglu. Neural discrete representation learning. In *Advances in Neural Information Processing Systems (NeurIPS)*, 2017.
- [67] Georgios Vardakas and Aristidis Likas. Neural clustering based on implicit maximum likelihood. *Neural Computing and Applications*, 35(29):21511–21524, 2023.
- [68] Ramakrishna Vedantam, Arthur Szlam, Maximilian Nickel, Ari Morcos, and Brenden M. Lake. CURI: A benchmark for productive concept learning under uncertainty. In *International Conference on Machine Learning (ICML)*, 2021.
- [69] Bowen Wang, Liangzhi Li, Yuta Nakashima, and Hajime Nagahara. Learning bottleneck concepts in image classification. In *Conference on Computer Vision and Pattern Recognition (CVPR)*, 2023.
- [70] Taylor Whittington Webb, Ishan Sinha, and Jonathan D. Cohen. Emergent symbols through binding in external memory. In *International Conference on Learning Representations (ICLR)*, 2021.
- [71] Antonia Wüst, Wolfgang Stammer, Quentin Delfosse, Devendra Singh Dhami, and Kristian Kersting. Pix2code: Learning to compose neural visual concepts as programs. *CoRR*, abs/2402.08280, 2024.
- [72] Yue Yang, Artemis Panagopoulou, Shenghao Zhou, Daniel Jin, Chris Callison-Burch, and Mark Yatskar. Language in a bottle: Language model guided concept bottlenecks for interpretable image classification. In *Conference on Computer Vision and Pattern Recognition (CVPR)*, 2023.
- [73] Chih-Kuan Yeh, Been Kim, Serkan Ömer Arik, Chun-Liang Li, Tomas Pfister, and Pradeep Ravikumar. On completeness-aware concept-based explanations in deep neural networks. In *Advances in Neural Information Processing Systems (NeurIPS)*, 2020.
- [74] Chih-Kuan Yeh, Been Kim, Serkan Ömer Arik, Chun-Liang Li, Tomas Pfister, and Pradeep Ravikumar. On completeness-aware concept-based explanations in deep neural networks. In *Advances in Neural Information Processing Systems (NeurIPS)*, 2020.
- [75] Richard Zhang, Phillip Isola, Alexei A Efros, Eli Shechtman, and Oliver Wang. The unreasonable effectiveness of deep features as a perceptual metric. In *Proceedings of the IEEE conference on computer vision and pattern recognition*, 2018.

Supplementary Materials

In the following, we provide details on Neural Concept Binder, experimental evaluations as well as additional evaluations.

Impact Statement

Our work provides a new framework for unsupervised concept learning for visual reasoning. It improves the reliability of the unsupervised concept learning by explicitly including both inspection and revision of the concept space in the framework. NCB thus makes an important step towards more reliable and transparent AI, by providing an interpretable symbolic concept representation. This representation can be utilized within reliable and proven symbolic methods, or to improve transparency of neural modules. However, as the concepts are learned unsupervised, one has to keep in mind that they are not necessarily aligned with human knowledge, and might require inspections to achieve this. As NCB features a concept revision via human feedback, it is also necessary to consider that these revisions could have negative effects. A user with malicious intents could modify the memory and thus make the concept space incorrect. The fact that the learned representation of NCB is explicitly inspectable can, however, prove to be helpful in limiting such malicious interventions.

A Details on Neural Concept Binder

A.1 Selection Function

In the default setting, NCB selects that encoding from the retrieval corpus with the minimal distance to infer a corresponding concept representation. We further explore a top- k approach for the selection function s with $k > 1$. In this case, s selects the values v_l , for the $k \in \mathbb{N}$ closest encodings in the retrieval corpus and the resulting c_i^j is obtained via majority vote over these values. Additionally, via this selection approach the probability of c_i^j based on the occurrence distribution over the top- k values v_l can be estimated. We provide ablations regarding this in our evaluations in Suppl. F.1.

Algorithm 1 Training NCB: Given a set of images, X , a block-slot encoder, g_θ , an unsupervised clustering model h_ϕ .

1: $\hat{\theta} \leftarrow \text{fit}(g_\theta, X)$	▷ Step 1: Optimize the block-slot encoder
2: $Z \leftarrow g_{\hat{\theta}}(X)$	▷ Step 2.1: Gather block-slots from optimized g
3: $\bar{Z} \leftarrow \text{select_object_slots}(Z)$	▷ Step 2.2: Filter out <i>non-object</i> slots
4: for $j \in \{1, \dots, N_B\}$ do	
5: $\hat{\phi}^j \leftarrow \text{fit}(h, \bar{Z}^j)$	▷ Step 2.3: Obtain clustering of \bar{Z}^j
6: $R^j \leftarrow \text{distill}(\hat{\phi}^j, \bar{Z}^j)$	▷ Step 2.4: Extract clustering representation into \mathcal{R}^j

A.2 Details on Training

The first step (cf. L.1 in Alg. 1) optimizes the encoder g to provide *object-factorised* block-slot encodings. It is optimized for unsupervised image reconstruction based on the decoder model, $g'_\theta : z \rightarrow \tilde{x} \in \mathbb{R}^D$ (cf. Fig. 2) and a mean squared error loss: $L = L_{\text{MSE}}(x, g'(g(x)))$. In practice, additional losses have been shown to be beneficial for further improving the obtained block-slot encodings [56, 55].

The goal of NCB’s second training step is to obtain the retrieval corpus, \mathcal{R} . This procedure is based on obtaining an optimal clustering of block encodings via an unsupervised clustering model h and distilling the resulting information from h into explicit representations in the retrieval corpus. This step is divided into several substeps (cf. L.2-6 in Alg. 1). It starts with gathering a set of block-slot encodings $Z = g_{\hat{\theta}}(X)$. As Z can include slots which do not encode objects but, e.g., the background, we first select the "object-slot" encodings from Z . This step results in $\bar{Z} \subseteq Z$ and consists of a heuristic selection based on the corresponding slot attention masks (described in the following section).

For each block j we next perform the following steps: (i) a clustering model, h_{ϕ^j} (cf. Fig. 2), is fit to find a set of clusters within \bar{Z}^j thereby identifying $N_C \in \mathbb{N}$ meaningful clusters. The learning of this optimal clustering is based on an unsupervised criteria, *e.g.*, density based scores [44]. Ideally, this leads to that objects that share similar block encodings are clustered together in the corresponding latent block space, whereas objects that possess very different block encodings are associated with distant clusters. This resulting clustering is stored in h ’s internal representation which we denote as ϕ^j (*e.g.*, the merge tree in a hierarchical clustering method [8, 9, 45]). Importantly, h_{ϕ^j} is optimized individually for each block. (ii) In the `distill` step representative block encodings of each cluster, enc^j , are extracted from h ’s internal representation, ϕ^j . Hereby, every enc^j can represent either an averaged *prototype* or instance-based *exemplar* encoding of a cluster. This is performed for every identified cluster, $v \in \{1, \dots, N_C\}$ and is based on \bar{Z}^j and ϕ^j . As a result, the tuples (enc^j, v) are explicitly stored in the retrieval corpus \mathcal{R}^j . The final retrieval corpus consists of the set of individual corpora for each block, $R = [R^1, \dots, R^{N_B}]$.

We note that in practice, it is further possible to finetune the block-slot encoder, g , through supervision from the hard binder, *e.g.*, once initial categories have been identified and can be achieved via a standard supervised approach. Ultimately, this allows for *dynamically* finetuning NCB’s concept representations.

Heuristic object-slot selection. In the following we describe the process of identifying the slot which contains an object. This is based on heuristically selecting slot ids based on their corresponding slot attention values. Importantly, this approach can select object-slot ids without additional supervision, *e.g.*, via (GT) object segmentation masks.

In principle, our object-slot selection approach finds the slots which contain slot attention values above a predefined threshold, $\delta \in (0, 1]$. However, selecting such a threshold can be cumbersome in practice. In our evaluations we therefore select only a single slot per image, *i.e.*, that slot which contains the maximum slot attention value over all slots. Essentially, this sets the maximum number of selected slots per image to 1 and in images that contain one objects represent no loss of object relevant information. In preliminary evaluations we observed that the consensus between object-slot selection based on GT object segmentation masks (matching object segmentation masks with slot attention masks) and our maximum-based selection heuristic is 99.45% over 2000 single object images.

A.3 Instantiating Neural Concept Binder

We instantiate NCB’s soft binder via the SysBinder approach of Singh et al. [56] which has been shown to provide valuable, object-factor disentangled representations. Thus, the soft binder was trained as in the original setup and with the published hyperparameters. Furthermore we instantiate the clustering model, h , via the powerful HDBSCAN method [8, 9, 45] (based on the popular HDBSCAN library³). Hereby, h ’s internal representation, ϕ , consists of the learned hierarchical merge tree. In practice we found it beneficial to perform a grid search over h ’s hyperparameters based on the unsupervised density-based cluster validity score [44]. The searched parameters are the minimal cluster size (the minimum number of samples in a group for that group to be considered a cluster) and minimal sample number (the number of samples in a neighborhood for a point to be considered as a core point) each over the values [5, 10, 15, 20, 25, 30, 50, 80, 100]. Moreover, we utilize the excess of mass algorithm and allow for single clusters. We performed the training of the retrieval corpus, *i.e.*, fitting h , on a dataset of images containing single objects for simplifying the subsequent concept inspection mechanisms of our evaluations. However, this can easily be extended to multiple object images by utilising the soft binder’s slot attention masks to identify relevant objects in an image. Finally, we instantiate the retrieval corpus as a set of dictionaries and, unless stated otherwise, we utilise a retrieval corpus which contains one prototype and a set of exemplar encodings per concept. Furthermore, $s_{\mathcal{R}}$ represents the argmin selection function and we utilize the euclidean distance as $d(\cdot, \cdot)$. It is important to note that h does not make any assumptions about the number of clusters, N_C . Thus, although h fits a clustering to best fit the block-slot encodings of a block, it can potentially provide an overparameterized clustering, *e.g.* by representing one underlying factor such as “gray” with several clusters. This highlights the importance of task-alignment, *e.g.*, for symbolic downstream tasks, and concept inspection for general concept alignment. We refer to our code for

³<https://hdbscan.readthedocs.io/en/latest/index.html>

more details⁴, where we will publish trained model checkpoints and corresponding parameter logs upon acceptance.

A.4 Computational Resources

The resources used for training NCB were: CPU: AMD EPYC 7742 64- Core Processor, RAM: 2064 GB, GPU: NVIDIA A100-SXM4-40GB GPU with 40 GB of RAM. Hereby, training the SysBinder model [56] is the computational bottleneck of NCB where we utilised two GPUs per SysBinder run. Training for 500 epochs took ≈ 108 GPU hours. The fitting of h (including the grid search over hyperparameters) was performed on the CPU and finished within a few hours.

B Details on CLEVR-Sudoku

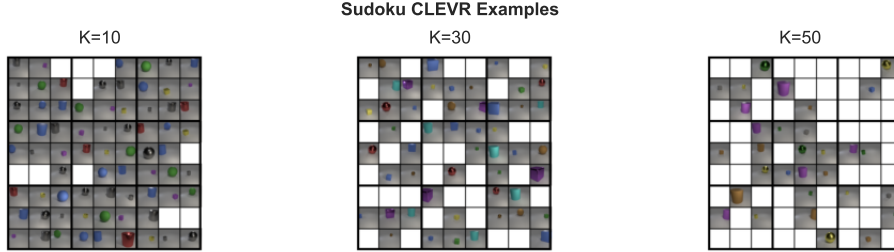


Figure 7: Examples of Sudoku CLEVR for different K values.

CLEVR-Sudoku provides Sudokus based on the datasets CLEVR and CLEVR-Easy. Classic Sudokus have a 9x9 grid which is filled with digits from 1 to 9. In CLEVR-Sudoku these digits are replaced by images of objects. Hereby, a digit corresponds to a specific attribute combination, *e.g.*, "yellow" and "sphere". Consequently, digits of the Sudoku are replaced by images of objects with these attribute combinations. These images each contain one object. To indicate, which attributes correspond to which digit, candidate examples of the digits are provided. The number of these examples is a flexible parameter, in our evaluations we used $N \in \{1, 3, 5, 10\}$. Further, the number of images provided in the Sudoku grid is flexible as well. In our main evaluations we only considered CLEVR-Sudokus with $K = 30$, meaning that 51 of the 81 Sudoku cells are filled and 30 are left to complete. For additional investigation we considered values for $K \in \{10, 50\}$ as well. Examples of those Sudokus for Sudoku CLEVR are shown in Fig. 7. The dataset has a number of 1000 samples for *Sudoku CLEVR-Easy* and *Sudoku CLEVR* respectively for each value of K . Each sample has a different puzzle and a distinct set of images, no image is used twice for one puzzle⁵.

C Datasets

CLEVR. Briefly, a CLEVR [24] image contains multiple 3D geometric objects placed in an illuminated background scene. Hereby, the objects can possess one of three forms, one of 8 colors, one of two sizes, one of two materials and a random position within the scene.

CLEVR-Easy. CLEVR-Easy [56] images are similar to CLEVR images, except that in CLEVR-Easy the size and material is fixed over all objects, *i.e.*, all objects are large and metallic.

CLEVR-Hans3. The CLEVR-Hans3 [59] represents a classification dataset that contains images with CLEVR objects where the image class is determined based on the attribute combination of several objects (*e.g.*, an image belongs to class 1 if it contains a large, gray cube and a large cylinder). Furthermore, we utilize a confounded and non-confounded version of CLEVR-Hans3. In the confounded case (*i.e.*, the original dataset) the train and validation set contains spurious correlations among object attributes (*e.g.*, all large cubes are gray in class 1) that are not present in the

⁴Code available here.

⁵The code for generating the dataset is available in our code repository, the already generated data files will be made public upon acceptance.

test set (*e.g.*, large cubes of class 1 take any color). In our evaluations investigating only neural-based classification we utilize the original validation split as the held-out test split and select a subset from the original training split as validation set. Thus, the non-confounded version corresponds to a standard classification setup in which the data distribution is identical over all three data splits. Lastly we provide evaluations on a single object version of CLEVR-Hans3 (class 1: a large, gray cube; class 2: a small metal cube; class 3: a large, blue sphere; *cf.* Tab. 3) and the original, multi-object version.

D Baseline Models

We note upfront, that all SysBind configurations below were trained for as many epochs as NCB, followed by an additional finetuning for 2 epochs on the same dataset that was used to distill NCB’s retrieval corpus.

SysBind (cont.). This denotes the original SysBinder configuration which was trained as in [56] and provides continuous block-slot encodings. We refer to the original work for hyperparameter details.

SysBind. This denotes a SysBinder configuration that was trained as in [56]. However, at inference time we perform discretisation via an argmin operation over the attention values to each block’s prototype codebook.

SysBind (hard). This denotes a configuration in which the SysBinder model was trained via a codebook attention softmax temperature of $1e - 4$, resulting in a learned discrete representation.

SysBind (step). SysBinder (step) is trained by step-wise decreasing this temperature his denotes a configuration in which the SysBinder model was trained via a step-wise decreasing codebook attention softmax temperature (with a decrease by a factor of 0.5 every 50 epochs, starting from 1.).

Supervised Concept Learner. This corresponds to a slot attention encoder [36] that was trained for set prediction (*i.e.*, in a supervised fashion) to predict the object-properties for every object in a CLEVR image. We refer to Locatello et al. [36] and Stammer et al. [59] for details.

E Details on Experimental Setup

E.1 Classifying object-properties from concept encodings

For our evaluations in the context of (Q1) we utilise a decision tree as classification model that is trained on a set of concept encodings to predict corresponding object properties, *e.g.*, *sphere*, *cube* or *cylinder*. Importantly, we train a separate classifier for each property category, *e.g.*, the categories *shape*, *color*, *material* and *size* in the case of CLEVR, and average accuracies over these. The classifiers parameters correspond to the default parameters of the sklearn library⁶.

E.2 CLEVR-Sudoku evaluations

For our CLEVR-Sudoku evaluations we use a solver that combines a symbolic classifier with a constraint propagation based algorithm. To solve CLEVR-Sudokus, it is at first required to detect the underlying mapping from the object attribute combinations to the digits via the provided candidate examples. For this, we require a symbolic classifier to learn this mapping, which in the case of our evaluations is achieved via a decision tree classifier. For each evaluated model the concept encodings of the candidate example images of a CLEVR-Sudoku are retrieved and provided as input to the classifier. Hereby, the corresponding digits are the labels to be predicted. With the predictions of the trained classifier the concept encodings of the images in the Sudoku grid are classified to get a symbolic representation of the Sudoku, *i.e.*, map the images in the cells to their corresponding digits. Based on this numerical representation of the puzzle, we use an algorithm from [46] that uses a combination of constraint propagation [6] and search. The algorithm keeps track of all possible values for each cell. Within each step, the Sudoku constraints are used to eliminate all invalid digits from the possibilities. Then the search of the algorithm select a digit for a non-filled cell. Based on this digit, the possibilities are updated for all other cells. When there is a constraint violation, the search-tree is traversed backwards and other possible digits for non-filled cells are explored. This process is

⁶<https://scikit-learn.org/stable/modules/generated/sklearn.tree.DecisionTreeClassifier.html>

repeated until the Sudoku is solved (in case the initial state inferred from the objects was correct) or until there is no possible solution left (meaning that the initial state was incorrectly inferred from the objects). The implementation of the algorithm is based on the code from⁷. Finally, to avoid errors due to random seeding of the classifier, for each puzzle we fit 10 independent classifiers (each with different seeds) to predict the corresponding mapping. For the results in our evaluations we average the performance over these 10 classifier seeds.

Lastly, the evaluations in the context of (Q2) are based on the trained (NCB) models of (Q1).

E.3 Obtaining Revisory Feedback

We note that the evaluations in the context of (Q3) are based on the trained NCB models of (Q1).

Revisory feedback for downstream Sudoku task.

To revise its discrete concepts, NCB offers the possibility to delete or merge clusters in the blocks. In the case of merging, the prototypes and exemplars of the clusters to be merged get aggregated so that they all map to the same concept symbol. For deletion there are several processing cases, depending on how many categories are in the block and how many are supposed to be deleted:

- Case 1: if all clusters from a block should be deleted (or if there is only one concept in the block, which should be deleted), we map all samples to the same concept. This results in the block containing no information (we keep the block to avoid issues with the dimensions of the concept representation).
- Case 2: all clusters but one are to be deleted. In this case we still want to distinguish between the presumably "informative" cluster and the uninformative other clusters. Therefore we map all the blocks to be deleted to one cluster id instead of deleting them completely.
- Case 3: at least two clusters should not be deleted. In this case, we remove the encodings of these clusters completely. The cluster id for these clusters then no longer exist in the retrieval corpus.

Feedback via GPT-4. We systematically prompt GPT-4 [47] for receiving revisory feedback. We provide example prompts in Listing 1. First, we ask GPT-4 to name relevant object properties for a set of example images, *e.g.*, "shapes: [cube, cylinder], color: [red, blue]". Based on these provided property lists we ask GPT-4 to provide a descriptive list of each exemplar object's image for each concept of each block, *e.g.*, "{Exemplar1: [cube, red], Exemplar2: [cube, blue], ... }". Based on these descriptions we identify whether all exemplar objects of one concept share a common subproperty, *e.g.*, "cube". If there is no common subproperty, the concept should be removed from the retrieval corpus. In a second step we evaluate whether all exemplar objects from two separate concepts share a common subproperty. In this case we decide to merge the concepts based on GPT-4's analysis. We finally integrate GPT-4's feedback into NCB's retrieval corpus via the procedures described above.

Feedback via simulated humans. To simulate feedback by a human user, we utilise a decision tree (DT) classifier to classify attributes of objects based on NCB's discrete concepts (similar to Q1). For this, we transform the concept-slot encodings into multi-hot encodings. We then extract the importance of the concepts from the trained DT classifier. Based on this we select "unimportant" concepts to be deleted based on the procedures describe above. Note that in this setting we do not query for feedback considering the merging of concepts.

E.4 Neural Classification

We note that the evaluations in the context of (Q4) are based on the trained NCB models of (Q1).

Neural classifier. In the context of the classification evaluations (Q4) we utilize the setup of Stammer et al. [59]. Specifically, a set transformer [31] is trained to classify images from the CLEVR-Hans3 dataset given encodings that are, in turn, obtained from either NCB or a supervised trained slot attention encoder [36] (SA). In the case of utilizing NCB's encodings we transform the concept-slot encodings into multi-hot encodings to match those of the SA-based setup. We refer to Stammer et al. [59] and our code for additional details concerning this setup.

⁷<https://github.com/ScriptRaccoon/sudoku-solver-python/tree/main>

Table 4: Classifying attributes from concept representations. Best results are in bold.

N Train	SysBinder [cont.]	SysBinder	SysBinder (hard)	SysBinder (step)	NCB (P)	NCB (P+E)	NCB (P+E, topk)
— CLEVR-Easy —							
N=2000	99.83±0.24	92.49±5.45	22.92±0.00	95.76±4.92	98.76±1.05	99.02 ±1.00	98.93±1.10
N=200	99.20±0.41	87.90±8.05	22.92±0.00	92.42±7.32	97.11±2.16	98.50 ±1.80	98.42±1.91
N=50	91.13±4.21	78.41±8.69	22.92±0.00	70.64±11.89	94.31±4.47	95.87 ±2.93	95.72±3.04
N=20	64.88±10.89	62.61±7.18	22.92±0.00	54.61±9.57	90.50±7.09	94.22 ±4.11	94.15±4.14
— CLEVR —							
N=2000	98.86±1.15	86.22±10.40	36.46±0.00	88.90±14.81	96.77±2.63	97.26 ±2.67	97.17±2.68
N=200	97.61±2.58	81.13±12.39	36.46±0.00	83.17±17.05	96.41±2.64	96.80 ±3.01	96.80±3.04
N=50	93.25±4.62	61.67±8.51	36.46±0.00	68.81±17.74	94.29±4.78	94.67 ±4.65	94.10±5.25
N=20	79.11±8.75	49.79±6.73	36.46±0.00	58.58±16.09	87.55±5.35	88.57 ±4.68	88.42±4.63

Table 5: Ablation: Classifying attributes from concept representations with sub-optimal NCB components. The left column serves as a reference and represents the configurations used in the main evaluations, *i.e.*, where the soft binder was trained for 600 epochs and the clustering model represented the HDBSCAN approach that was optimized via a grid-search over its corresponding hyperparameters.

N Train	NCB	NCB (50 epochs)	NCB (100 epochs)	NCB (w/o grid search)	NCB (kmeans)
— CLEVR —					
N=2000	97.26±2.67	95.19±1.2	94.91±3.45	97.69±2.95	97.26±2.80
N=200	96.80±3.01	93.69±1.08	93.83±2.90	96.80±3.09	96.01±3.51
N=50	94.67±4.65	89.10±4.29	89.67±6.95	94.46±5.65	87.65±8.78
N=20	88.57±4.68	83.46±6.08	88.48±2.36	90.51±4.40	73.52±10.92

Obtaining explanations from the neural classifier. We provide the explanations in Tab. 3 for the single object version of Fig. 14. To obtain these explanations for the neural classifier we utilize the approach of Stammer et al. [59] which is based on the integrated gradients explanation method [61]. This estimates the importance value of each input element (in this case input concept encodings) for a classifiers final decision. We remove negative importance values and normalise the importance values as in [59]. We then sum over the importance values corresponding to images of a class, normalise the values per block and binarize these aggregated and normalised importance values via the threshold of 0.25 (*i.e.*, importance values above 0.25 are set to 1, otherwise 0). This provides us with a binary vector indicating which concepts are considered important per block. We illustrate these investigations via explanations from one model.

Explanatory interactive learning (XIL). Explanatory interactive learning (+ *XIL on NN*) is used to mitigate the confounder in the CLEVR-Hans dataset. Hereby, (simulated) human feedback on the explanation of the neural classifier is used to retrain the classifier via the loss based approach of Stammer et al. [59]. The feedback annotations mark which of NCB’s concepts should *not* be used for the NN’s classification decision. This is integrated into the NN by training the model to provide (integrated gradients-based) explanations that do not focus on these concepts. We refer to Stammer et al. [59] for details. The second form of interactive learning (+*XIL on NCB concepts*) is directly applied on the NCB’s concept representation. Specifically, concepts from NCB that encode information concerning the irrelevant, confounding factors are simply set to zero, corresponding to *not being inferred for the object in the image*. *E.g.*, if the NCB infers concepts concerning the color “gray” to be present in an object and the underlying confounder is the color “gray” the corresponding concept activations of the NCB’s prediction are set to zero, *i.e.*, no gray. Then the neural classifier is retrained on the new concept representations. Next to a better performance, the advantage of this approach is that it does not require the more costly loss-based XIL training loop. We illustrate these investigations via interactions on one model.

F Additional Quantitative Results

F.1 Encoding Expressivity

In our evaluations in Tab. 2 it appears that training for discrete encodings via *SysBinder (hard)* leads to no learning effect of the model altogether. In contrast training step-wise via *SysBinder (step)*

provides better results, even slightly above the encodings of *SysBinder* (*i.e.*, training for continuous representations and then discretising via argmin). Lastly, we observe that NCB’s encodings lead to much lower performance variance compared to all baselines. Particularly *SysBinder (step)*’s high variances, hint towards issues with local optima.

We further provide ablations in the context of (Q1) on different model choices of NCB in Tab. 4. Specifically, we investigate the effect of a top- k selection function as well as the influence of using only prototype encodings in the retrieval corpus (NCB (P)) versus using prototype *and* exemplar encodings (NCB (P+E)). Unless noted otherwise, the NCB configurations in Tab. 4 utilize the argmin selection function. We note that when using prototypes, the average encoding of all elements in a cluster is formed, resulting in one prototype encoding per cluster in R^j . In the second variant, we extend the prototypes with exemplars for each cluster. Exemplars are representative encodings for this cluster added to the corpus, resulting in a larger corpus, which potentially provides an improved structure of the encoding space. Indeed, we observe that NCB provides best performances via the argmin selection function and utilising both prototype and exemplar encodings. This was the setting used in all evaluations of the main paper.

F.2 Ablation Analysis of Suboptimal NCB Components

Lastly, in the context of (Q1) we further refer to ablations in Tab. 5 on the specific implementation choices of the NCB instantiation of our evaluations. We hereby investigate the effect of sub-optimal soft and hard binder components on a classifier’s ability to identify object attributes from NCB’s concept encodings. Specifically, we investigate (i) the effect when the soft binder, *i.e.*, *SysBinder* encoder, was trained for fewer epochs, resulting in less disentangled continuous representations, and (ii) when the HDBSCAN model of the hard binder was not optimized via a parameter grid search or replaced with a more rudimentary clustering model, *i.e.*, a k-means clustering approach [38].

In the leftmost column of Tab. 5, we provide the performances of the NCB configuration of our main evaluations as a reference. As a reminder, hereby, NCB’s soft binder was finetuned for 600 epochs, and its hard binder component contains a clustering model based on the HDBSCAN approach that was furthermore optimized via a grid search over its corresponding hyperparameters. Focusing on the next two columns right of the baseline, we observe that when the soft binder component is trained for fewer epochs than the baseline NCB we indeed observe a decrease in classification performance. Notably, however, we still observe higher performances in comparison to the discrete *SysBinder* configurations (*cf.* Suppl. F.1), but also when compared to *SysBinder*’s continuous configuration (for $N = 20$). Focusing next on the rightmost column of Tab. 5 where NCB’s clustering model was replaced with the more rudimentary k-means clustering approach, we observe a strong decrease in classifier performance. This is particularly true in the small data regime ($N = 50$ and $N = 20$). Surprisingly, focusing on the second to the rightmost column, we observe that when we select the default hyperparameter values of the HDBSCAN package (rather than performing a grid-search over these), the classifier reaches slightly improved performances than via the baseline NCB configuration (particularly for $N = 20$). Thus, in this particular case, the default values seem practical. However, this cannot be guaranteed in all future cases, and we still recommend performing a form of grid search if no prior knowledge can be provided upfront on an optimal parameter set. We postulate that the specific density-based cluster validity score used for selecting the optimal cluster parameters has been sub-optimal and leave investigating other, more optimal selection criteria for future work.

Overall, our ablation investigations indeed indicate that we obtain less expressive concept encodings via NCB with less powerful sub-components. However, we also observe a certain amount of robustness of our NCB instantiation towards sub-optimal components.

F.3 Analysis of Learned Concept Space

We here provide a brief analysis of NCB’s learned concept space. These evaluations were performed on the models that were trained in the context of (Q1). Specifically, in Fig. 8, we provide the number of obtained concepts over all blocks (averaged over the 3 initialization seeds) both for CLEVR-Easy and CLEVR. We observe a much larger number of concepts overall for the CLEVR dataset but also a much larger variance in the number of concepts. This is largely due to that in CLEVR-Easy $N_B = 8$ whereas in CLEVR $N_B = 16$. Thus, the models are able to learn a more overparameterized concept space in the case of CLEVR. Further, in Fig. 9, we present the

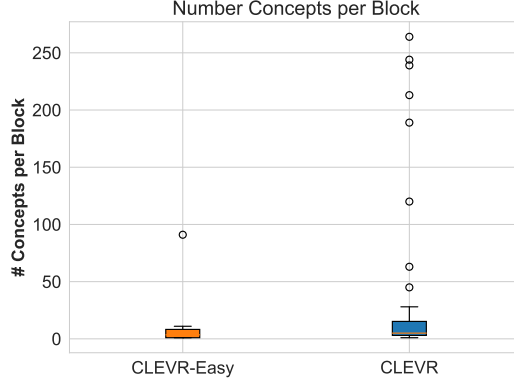


Figure 9: The distribution of number of obtained concepts per block both for CLEVR-Easy and CLEVR. These values are computed over all seeds.

distribution of the number of concepts per block over all 3 NCB runs, both for CLEVR-Easy and for CLEVR. We observe that while most blocks contain maximally 20 concepts for CLEVR-Easy and 50 for CLEVR, there are several block outliers which contain a much greater set of concepts. These represent cases in which the initial block-slot encoding space was uninformative to begin with and, therefore, difficult to find some form of useful clustering via h . Where some of these blocks only contained irrelevant information in general, some blocks encoded positional information, which represents a continuous variable to begin with and is thus unlikely to be well represented via a clustering.

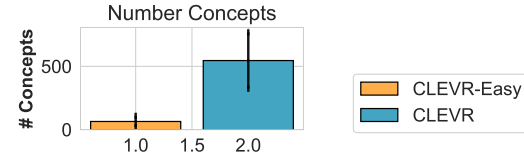


Figure 8: Average number of concepts in NCB’s retrieval corpus.

F.4 CLEVR-Sudoku Evaluations

In our evaluations on (Q2) we observe that, interestingly, for Sudoku CLEVR the supervised object classifier shows better results than for CLEVR-Easy. This seems counter-intuitive, however, in CLEVR-Easy-Sudoku digit labels are mapped to combinations of attributes that only stem from two categories, shape and color (in contrast to four categories in CLEVR-Sudoku) thus making it more likely to obtain recurring attributes over several digits (*e.g.*, digits 3, 4 and 5 of Fig. 4 all depict green objects). Thus, if an error occurs in the digit classification due to errors concerning one attribute the effect of this error will have a larger effect. Moreover in the case of CLEVR-Easy, we observe that in comparison to the supervised model, whose property misprediction errors can lead to large issues in the downstream module, NCB’s unsupervised and somewhat overparameterised concept space appears to dampen this issue, thus leading to a higher number of solved puzzles, *e.g.*, for 3, 5 or 10 examples.

In Fig. 10 we report the errors in predicting the underlying digits of the CLEVR-Sudokus. We observe that the errors of *SysBinder (unsupervised)* are drastically higher than the errors of the other methods. These high classification errors further explain this method’s low performances, *i.e.*, did not allow to solve any Sudoku. It can further be seen that for one example per digit the digit classification errors are much higher. This is reasonable as hereby the difficulty for the classifier is also higher. However, with an increasing number of examples the classifier’s errors decrease. The relations between the errors in the digit prediction and the overall performance in CLEVR-Sudoku are similar which is sensible since the error is decisive for the number of solved puzzles.

We further evaluate the influence of the number of missing images per Sudoku. For this we consider Sudokus with $K \in \{10, 30, 50\}$. The results on these variations with 5 candidate example images are reported in Fig. 11. We see that the more empty cells there are in a Sudoku’s initial state (higher K), the more Sudokus are solved. This is due to the lower probability of misclassifying an image

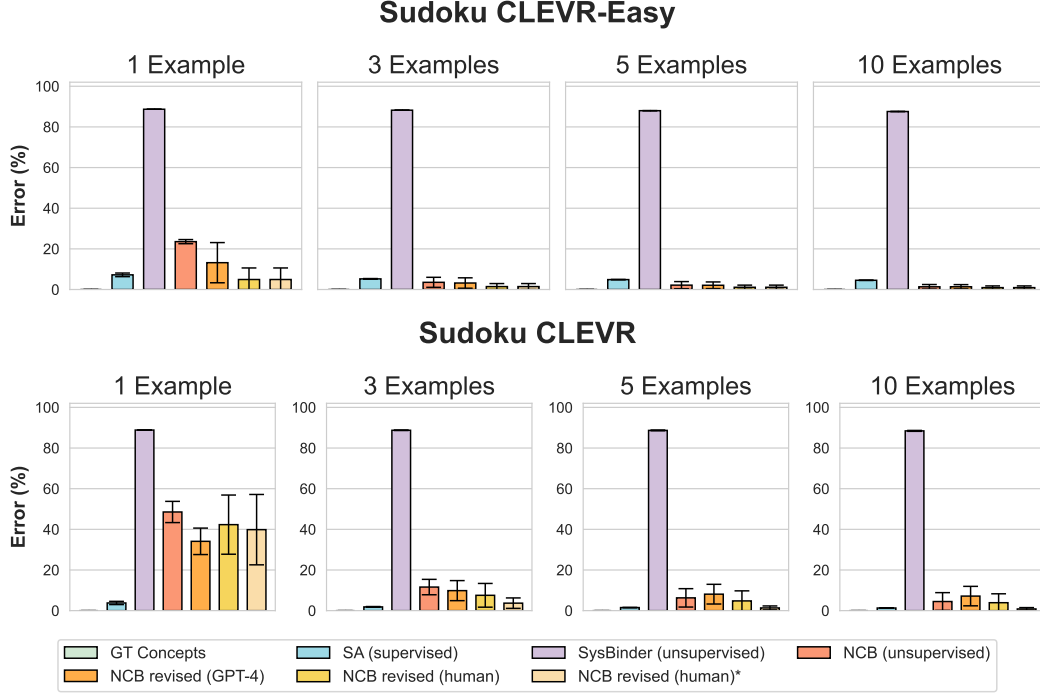


Figure 10: Error ratios (%) of the digit classification in CLEVR-Sudoku based on different symbolic concept encodings.

inside the Sudoku cells, as there are less images to classify. This pattern is observable for all of the different concept encodings we compared.

F.5 Revision Statistics

We provide statistics of the number of resulting removal requests per agent in Fig. 12. For the revision of CLEVR-Easy concepts we can see that GPT-4 detects only a few concepts to delete while via simulated human revision more concepts get deleted. In our initial evaluations (*cf.* Fig. 4) we had observed that human revision leads to substantial improvements while GPT-4’s revision even reduces performances slightly. For CLEVR-Sudoku in Fig. 12, we specifically observe that the overall number of deletions via GPT-4 is significantly higher. Interestingly, GPT-4 detects on average more blocks to delete here but also has a higher variance over the 3 different NCB runs. We hypothesize that this very “conservative” revision leads to the removal of concepts that actually contain valuable concept information, thus leading to less expressive concept encodings overall. Ultimately, this is due to mistakes in GPT-4’s analysis of provided images (*cf.* Suppl. E.3).

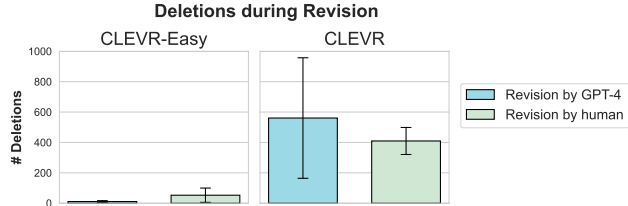


Figure 12: Average number of cluster deletions over all blocks via GPT-4 and simulated human user revision.

F.6 Dynamically Discretising Continuous Factors via Symbolic Revision

In our second set of evaluations in the context of (Q3) we investigate the third form of symbolic revision as introduced in Sec. 3.3: adding concept information to the hard binder’s retrieval corpus. Hereby, we focus on the task of learning a novel concept that had only been stored implicitly in the soft binder’s representations, but not explicitly in the hard binder’s representations. Specifically, we focus on positional concepts of CLEVR objects where the underlying GT position is

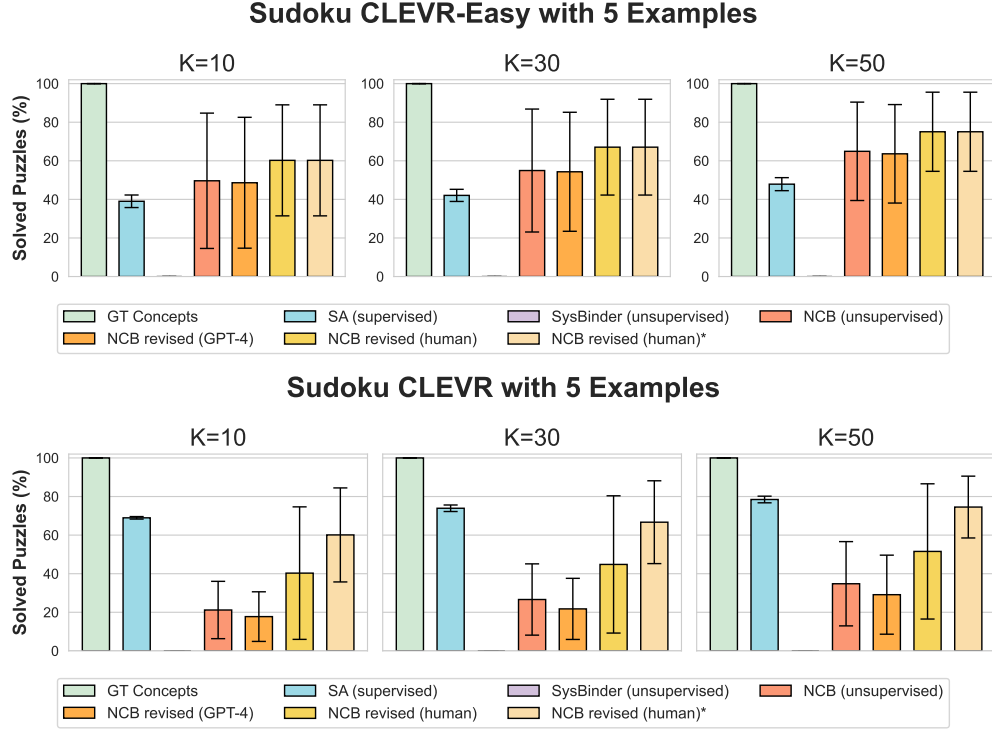


Figure 11: Solved Sudokus (%) of Sudoku CLEVR-Easy and Sudoku CLEVR with different values for K (empty cells).

represented via continuous values. Overall, it is debatable whether one, in principle, should or even can represent such a continuous underlying feature via a discrete concept representation. In this set of evaluations we investigate a setting in which it is necessary to identify coarse categorisations of an object’s position, *e.g.*, whether the object is placed in the left or right half of an image. We hereby simulate a human stakeholder that, having identified the block j that generally encodes position information, revises the corresponding concept encodings. This revision is performed in two ways: (i) by iterating over all of the block’s concepts and merging concepts into left and right concepts or (ii) by replacing all information in \mathcal{R} with encodings from a selected set of positive example images for the two relevant positions. Fig. 13 presents the results of training a classifier to predict the attributes “left” and “right” from NCB’s encodings (we here focus only on one seeded run for illustrations) with different types of revision. We observe that both allow to easily retrieve relevant information from NCB’s newly revised concept space. These results illustrate the important ability to easily adapt the hard binder’s concept representations by *dynamically re-reading* out the information of the soft binder’s representations in a use-case based manner. The results further illustrate the effect of adding prior knowledge to NCB’s concept representations, thereby potentially reducing the amount of inspection effort required on the stakeholder’s side, *e.g.*, in comparison to the merge revision.

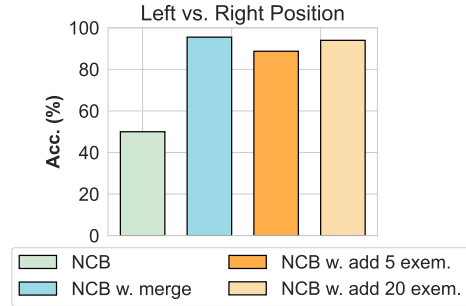


Figure 13: Test accuracy (%) for classifying objects as placed left or right in a scene.

F.7 Classifying CLEVR-Hans3

In our final evaluations (Q1) we highlight the advantage of NCB’s concept encodings when combined with *subsymbolic* (*i.e.*, neural) modules for making their decisions transparent.

Specifically, while a discrete concept representation is technically not required for neural modules, it has a key advantage: a discrete and inspectable representation allows for transparent downstream computations. We highlight this property in the context of image classification on variations of the benchmark CLEVR-Hans3 dataset [59]. For these evaluations we revert to training a set transformer [31] (denoted as *NN* in the following) for classifying images when provided the unsupervised concept encodings of NCB as image representations. We denote this configuration as *NCB + NN* and compare it to a configuration in which the set transformer is provided concept encodings from a supervised slot attention encoder, denoted as *SA + NN*. In Fig. 14 we observe that NCB’s concepts perform on par with those learned supervisedly, each reaching held-out test accuracies higher than 95%.

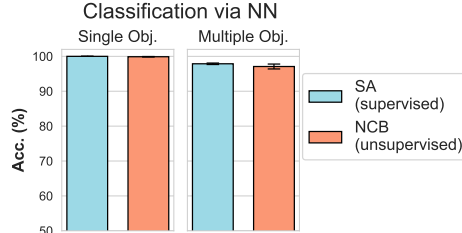


Figure 14: Test accuracy (%) for classifying CLEVR-Hans3 images with a neural classifier that is provided concept representations of NCB and of a supervised trained slot attention encoder. We differentiate here between class rules based on one object and multiple objects.

F.8 Confounding Evaluations

For the confounding mitigation evaluations in the context of (Q4) we train the *NCB + NN* configuration on the confounded version of CLEVR-Hans3, where we hereby focus on the single object class rules similar to those in Fig. 14. In this case all large cubes of class one images possess the color gray at training time, but arbitrary colors at test time. We observed accuracies of *NCB + NN* on the confounded validation set of 99.22% against the non-confounded test set 79.29%. This very high validation accuracy versus a significantly reduced test accuracy indicates that the classifier is strongly influenced by the datasets underlying confounding factor.

G Qualitative Results

Fig. 15 and Fig. 16 represent qualitative inspection results of NCB’s learned concepts. We specifically present implicit inspection via exemplars of concepts from two blocks from NCB when trained on CLEVR-Easy. One can observe that block 2 (Fig. 15) appears to encode shape concepts, however contains one ambiguous concept. We further observe that Fig. 16 appears to encode color concepts, whereby it contains one ambiguous concept (concept 8) and two concepts that appear to both encode the color purple (concept 9 and 10) which could potentially be merged.

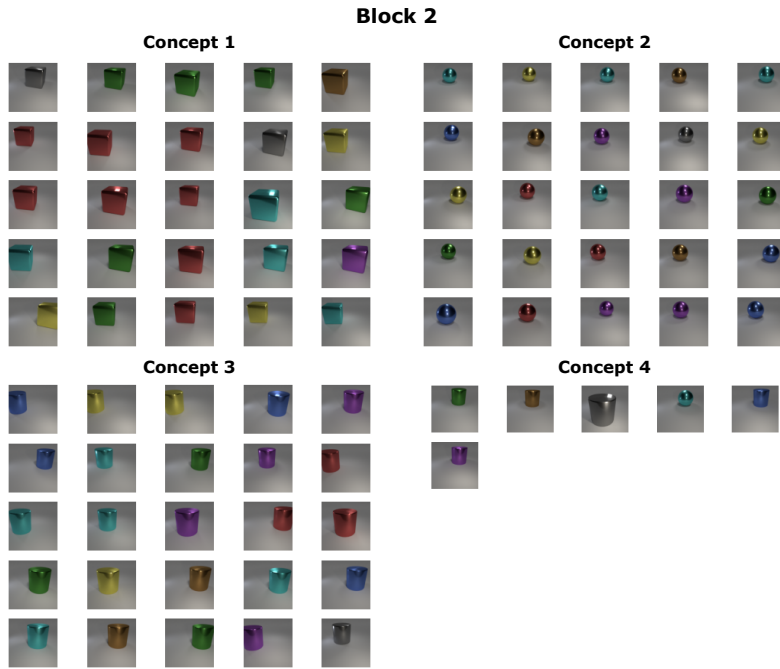


Figure 15: Concepts of Block 2 for NCB with CLEVR-Easy. We here provide implicit inspection examples (*i.e.*, via exemplars of each concept). We observe that block 2 appears to encode shape information (concept 1-3) and contains one ambiguous concept (concept 4).

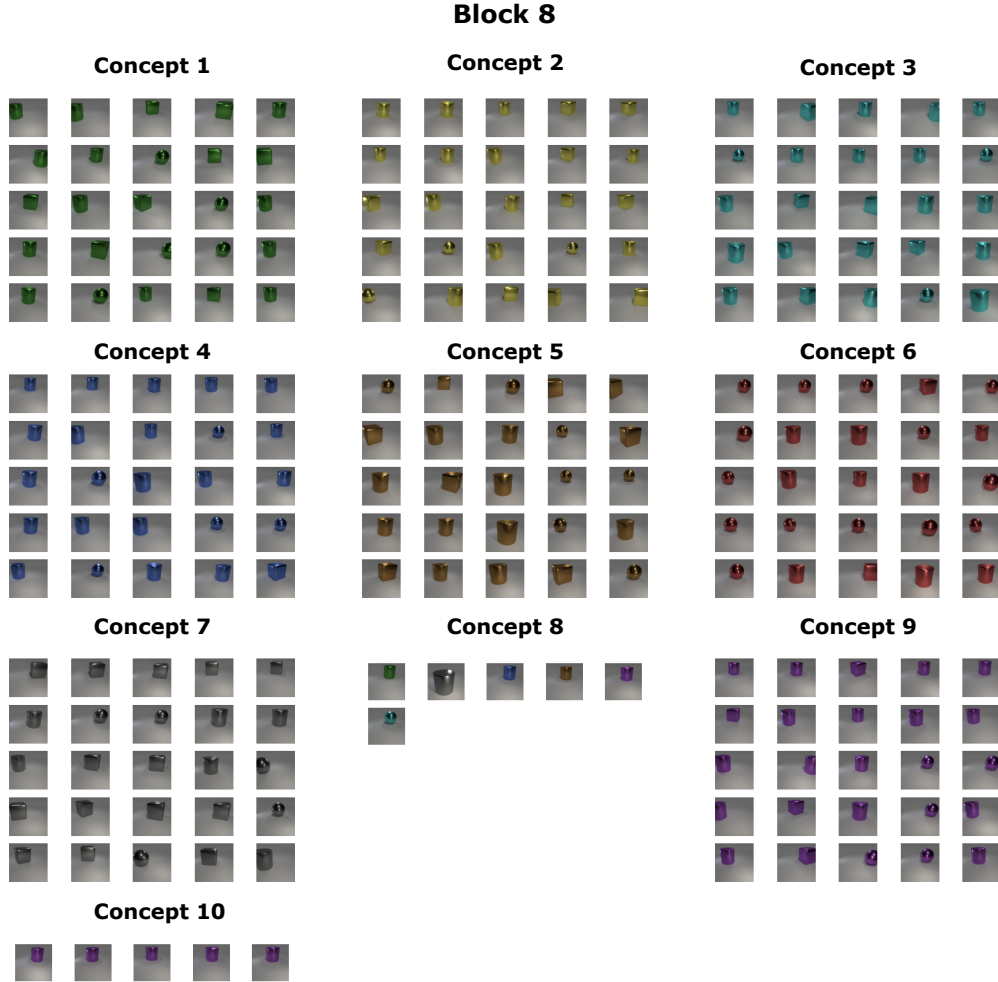


Figure 16: Concepts of Block 8 for NCB with CLEVR-Easy. We here provide implicit inspection examples (*i.e.*, via exemplars of each concept). We observe that block 8 appears to be encoding color information, contains one ambiguous concept (concept 8) and two concepts that appear to both encode the color purple (concept 9 and 10).

Table 6: Percentage of solved CLEVR-Sudokus for different number of example images.

Sudoku CLEVR-Easy	1 Example	3 Examples	5 Examples	10 Examples
GT Concepts	100.0 \pm 0.00	100.00 \pm 0.00	100.00 \pm 0.0	100.00 \pm 0.00
SA (supervised)	35.22 \pm 5.63	40.07 \pm 3.76	42.07 \pm 3.14	44.36 \pm 2.54
SysBinder (unsupervised)	0.00 \pm 0.00	0.00 \pm 0.00	0.00 \pm 0.00	0.00 \pm 0.00
NCB (unsupervised)	6.13 \pm 4.42	47.30 \pm 33.06	54.95 \pm 31.86	63.21 \pm 27.45
NCB revised (GPT-4)	34.61 \pm 43.46	48.25 \pm 34.80	54.31 \pm 30.85	61.83 \pm 26.10
NCB revised (human)	54.41 \pm 37.40	64.00 \pm 28.53	67.07 \pm 24.83	70.10 \pm 21.52
NCB revised (human)*	50.81 \pm 45.38	62.00 \pm 34.78	66.40 \pm 30.38	70.43 \pm 26.35
Sudoku CLEVR				
GT Concepts	100.0 \pm 0.00	100.0 \pm 0.0	100.0 \pm 0.00	100.0 \pm 0.00
SA (supervised)	54.9 \pm 5.99	69.99 \pm 2.76	73.92 \pm 1.69	77.71 \pm 0.38
SysBinder (unsupervised)	0.00 \pm 0.00	0.00 \pm 0.00	0.00 \pm 0.00	0.00 \pm 0.00
NCB (unsupervised)	0.01 \pm 0.00	12.36 \pm 8.46	26.62 \pm 18.47	38.24 \pm 26.97
NCB revised (GPT-4)	1.11 \pm 1.19	16.18 \pm 11.93	21.76 \pm 15.84	27.75 \pm 20.14
NCB revised (human)	3.23 \pm 4.55	36.19 \pm 32.64	44.8 \pm 35.58	48.97 \pm 37.13
NCB revised (human)*	4.84 \pm 4.82	54.0 \pm 25.43	66.69 \pm 21.46	72.68 \pm 19.53

Table 7: Error ratios on digit classification of CLEVR-Sudokus for different number of example images.

Sudoku CLEVR-Easy	1 Example	3 Examples	5 Examples	10 Examples
GT Concepts	0.00 \pm 0.00	0.00 \pm 0.00	0.0 \pm 0.00	0.0 \pm 0.00
SA (supervised)	7.23 \pm 0.89	5.25 \pm 0.16	4.89 \pm 0.09	4.55 \pm 0.09
SysBinder (unsupervised)	88.69 \pm 0.05	88.12 \pm 0.18	87.66 \pm 0.31	87.30 \pm 0.40
NCB (unsupervised)	23.57 \pm 1.02	3.55 \pm 2.47	2.16 \pm 1.74	1.35 \pm 1.13
NCB revised (GPT-4)	13.21 \pm 9.89	3.21 \pm 2.56	2.1 \pm 1.64	1.36 \pm 1.06
NCB revised (human)	4.94 \pm 5.68	1.45 \pm 1.49	1.12 \pm 1.05	0.95 \pm 0.83
NCB revised (human)*	6.55 \pm 6.37	1.79 \pm 1.73	1.31 \pm 1.24	1.06 \pm 1.00
Sudoku CLEVR				
GT Concepts	0.00 \pm 0.00	0.00 \pm 0.00	0.00 \pm 0.00	0.00 \pm 0.00
SA (supervised)	3.78 \pm 0.79	1.85 \pm 0.18	1.52 \pm 0.09	1.30 \pm 0.08
SysBinder (unsupervised)	88.81 \pm 0.03	88.67 \pm 0.03	88.68 \pm 0.1	88.71 \pm 0.11
NCB (unsupervised)	48.54 \pm 5.22	11.61 \pm 3.79	6.30 \pm 4.52	4.49 \pm 4.37
NCB revised (GPT-4)	34.10 \pm 6.51	9.85 \pm 4.93	8.11 \pm 4.85	7.16 \pm 4.79
NCB revised (human)	42.32 \pm 14.56	7.55 \pm 5.84	4.80 \pm 4.94	3.91 \pm 4.38
NCB revised (human)*	39.85 \pm 17.31	3.69 \pm 2.57	1.34 \pm 0.97	0.84 \pm 0.66

H Numerical Results

In our evaluations we presented the results on CLEVR-Sudoku in the form of bar plots. We refer to Tab. 6, Tab. 7 and Tab. 8 for the numerical values for the different variations of the dataset.

Table 8: Percentage of solved CLEVR-Sudokus for different values of K with 5 example images.

Sudoku CLEVR-Easy	K=10	K=30	K=50
GT Concepts	100.0 \pm 0.00	100.0 \pm 0.00	100.0 \pm 0.00
SA (supervised)	39.02 \pm 3.25	42.07 \pm 3.14	47.89 \pm 3.37
SysBinder (unsupervised)	0.00 \pm 0.00	0.00 \pm 0.00	0.00 \pm 0.00
NCB (unsupervised)	49.64 \pm 35.07	54.95 \pm 31.86	64.91 \pm 25.50
NCB revised (GPT-4)	48.62 \pm 33.92	54.31 \pm 30.85	63.62 \pm 25.52
NCB revised (human)	60.23 \pm 28.77	67.07 \pm 24.83	75.05 \pm 20.51
NCB revised (human)*	60.50 \pm 35.24	66.40 \pm 30.38	73.39 \pm 24.96
Sudoku CLEVR			
GT Concepts	100.00 \pm 0.00	100.00 \pm 0.00	100.00 \pm 0.00
SA (supervised)	68.96 \pm 0.65	73.92 \pm 1.69	78.46 \pm 1.72
SysBinder (unsupervised)	0.00 \pm 0.00	0.00 \pm 0.00	0.00 \pm 0.00
NCB (unsupervised)	21.18 \pm 14.85	26.62 \pm 18.47	34.79 \pm 21.84
NCB revised (GPT-4)	17.76 \pm 12.86	21.76 \pm 15.84	29.12 \pm 20.49
NCB revised (human)	40.30 \pm 34.34	44.80 \pm 35.58	51.55 \pm 35.05
NCB revised (human)*	60.10 \pm 24.36	66.69 \pm 21.46	74.54 \pm 16.02

Listing 1: Prompts for GPT-4.

----- Property List Prompt:

You are provided six images. An image contains subimages. Each subimage depicts one object. Each object represents a reflective geometric solid that is placed in a neutral gray background scene with a light source. Furthermore, each object has multiple properties, e.g., color, shape, size, material. Each property can be subdivided into several sub-properties, e.g., brown is a sub-property of the property color.

Please provide a list of object properties and subproperties that are depicted in all images. Ignore the background and the object's luminance and reflectivity. Use the following answer template:

```
{  
property: [sub-property, sub-property, ...]  
property: [sub-property, sub-property, ...]  
...  
}
```

----- Description Prompt:

You are provided an image. The image contains at most 25 subimages. Each subimage depicts one object. Each object represents a reflective geometric solid that is placed in a neutral gray background scene with a light source. Furthermore, each object has multiple properties, e.g., color. Each property can be subdivided into several sub-properties, e.g., green is a sub-property of the property color. The possible properties and sub-properties are the following:

INSERT_PREVIOUSLY_OBTAINED_PROPERTY_LIST

Focusing only on these properties, please perform the following tasks. First, for every object in the image please list the sub-properties from the given lists that the object depicts. Only name the sub-properties that are given. Please use the following format:

```
{  
Object1: [sub-property, ...],  
Object2: [sub-property, ...],  
...  
}
```